haematologica
Journal of the Ferrata Storti Foundation

Menin inhibitor DS-1594b drives differentiation and induces synergistic lethality in combination with venetoclax in acute myeloid leukemia cells with rearranged mixed-lineage Leukemia and mutated nucleophosmin-1

by Valerio Ciaurro, Vassilena Sharlandjieva, Anna Skwarska, Catherine Chahrour, Natalia Baran, Zhihong Zeng, Cassandra Ramage, Naval Daver, Bing Z. Carter, Sovira Chaundhry, Palaniraja Thandapani, Maria Paola Martelli, Thomas A. Milne and Marina Konopleva

Received: December 2, 2024.
Accepted: October 31, 2025.

Citation: Valerio Ciaurro, Vassilena Sharlandjieva, Anna Skwarska, Catherine Chahrour, Natalia Baran, Zhihong Zeng, Cassandra Ramage, Naval Daver, Bing Z. Carter, Sovira Chaundhry, Palaniraja Thandapani, Maria Paola Martelli, Thomas A. Milne and Marina Konopleva. Menin inhibitor DS-1594b drives differentiation and induces synergistic lethality in combination with venetoclax in acute myeloid leukemia cells with rearranged MLL and NPM1 mutations.
Haematologica. 2025 Nov 6. doi: 10.3324/haematol.2024.286833 [Epub ahead of print]

Menin inhibitor DS-1594b drives differentiation and induces synergistic lethality in combination with venetoclax in acute myeloid leukemia cells with rearranged mixed-lineage Leukemia and mutated nucleophosmin-1

Valerio Ciaurro[1], Vassilena Sharlandjieva[2], Anna Skwarska[3], Catherine Chahrour[2], Natalia Baran[4,5], Zhihong Zeng[4], Cassandra Ramage[4], Naval Daver[4], Bing Z. Carter[4], Sovira Chaundhry[3], Palaniraja Thandapani[1], Maria Paola Martelli[6], Thomas A. Milne[2], Marina Konopleva[3,4]

[1] Department of Hematopoietic Biology and Malignancy, The University of Texas MD Anderson Cancer Center, Houston, TX 77030, USA

[2] MRC Molecular Haematology Unit, MRC Weatherall Institute of Molecular Medicine, Radcliffe Department of Medicine, University of Oxford, Oxford OX3 9DS, UK

[3] Department of Oncology, Albert Einstein College of Medicine, New York, 10461, USA

[4] Department of Leukemia, The University of Texas MD Anderson Cancer Center, Houston, TX 77030, USA

[5]Section of Experimental Hematology, Institute of Hematology and Transfusion Medicine, Warsaw, Poland

[6]Hematology and Clinical Immunology Section, Department of Medicine and Surgery, Center for Hemato-Oncological Research (CREO), University of Perugia, Perugia, Italy

Running head: DS-1594b and venetoclax in *MLL*r and *mtNPM1* AML

Corresponding author: Marina Konopleva, marina.konopleva@einsteinmed.edu_,718-430-2362

Contributions: V.C. designed and performed experiments, analyzed data, and wrote the manuscript; V.S. and A.S. contributed to experimental work and design, data analysis, and manuscript review; C.C. contributed to experimental work and design, as well as data analysis; N.B. contributed to experimental work and manuscript review; Z.Z. provided essential experimental tools and methodological guidance; C.R. and S.C. assisted with experimental work; N.D. provided clinical insights and contributed to manuscript review: B.C. provided cell lines and experimental support during revision; P.T. supported the project by facilitating experiments and providing reagents; M.P.M. and T.A.M. provided conceptual guidance, scientific discussions, and manuscript editing; and M.K. supervised the project, provided funding, and critically reviewed the manuscript.

Disclosures: T.A.M. is a paid consultant for and shareholder in Dark Blue Therapeutics Ltd. M.K serves on advisory boards for AbbVie, Auxenion GmbH, Dark Blue Therapeutics, Legend, MEI Pharma, Menarini/Stemline Therapeutics, Novartis, and Syndax. She also provides consulting for AbbVie, Adaptive, AmMax, Curis, Janssen, Kyowa Kirin, Menarini/Stemline Therapeutics, Novartis, Sanofi Aventis, Servier, and Vincerx. Additionally and has received research funding from AbbVie, Janssen, and Klondike Biopharma. N.D. reports receiving consultancy fees from Bristol-Myers Squibb, Daiichi, Pfizer, Gilead, Servier, Genentech, Astellas, AbbVie, ImmunoGen, Amgen, Trillium, Jazz, Syndax, Sumitomo, Kura, AROG, Servier, Shattuck labs, Sanofi, Arcellx, Caribou, Debiopharm, Aptos, Astra-Zeneca, StemLine, VincerX; research funding from Hanmi, Trovagene, FATE, Novimmune, Glycomimetics, BMS, Astellas, Daiichi, Abbvie, Immunogen, Shattuck labs, Sanofi, Arcellx, Caribou, Debiopharm, Aptos, Astra-Zeneca, StemLine, VincerX, Nerviano, FATE therapeutics, Sumitomo, Kura. M.P.M declares speaker honoraria/scientific advisory board consultancy for Abbvie, Amgen, Astellas, Be-One, BMS, Delbert, Gilead, Janssen, Jazz Pharmaceuticals, Novartis, Pfizer, Roche,

Servier. B.C. received research funding from REPARE Therapeutics and AmMax. P.T. in a scientific advisory board member at 65 Therapeutics.

Data-sharing statement: All high throughput data have been deposited in the Gene Expression Omnibus (GEO) under accession number GSE282741.

Acknowledgments: We thank Madison Semro, Associate Scientific Editor, and Dawn Chalaire, in the Research Medical Library at The University of Texas MD Anderson Cancer Center, for editing this article.

Funding: Founded by Daiichi Sankyo Co., Ltd.

ABSTRACT

Mixed-lineage leukemia *(MLL)* rearrangements and Nucleophosmin-1 (*NPM1)* mutations are associated with acute leukemias whose pathogenesis is critically influenced by protein-protein interactions between menin and MLL. We hypothesized that targeting the menin-MLL interaction using DS-1594b and blocking the antiapoptotic BCL-2 protein using venetoclax may promote differentiation and enhance eradication of *MLL*-rearranged and *NPM1*-mutated leukemias models. We treated acute myeloid leukemia (AML) cell lines with *MLL* rearrangements, *NPM1* mutations, other leukemias and primary samples from AML patients with venetoclax alone, DS-1594b alone, and their combination. We measured proliferation, viability, apoptosis, and differentiation using a variety of cellular assays, Western blotting, and BH3 profiling. Treatment with DS-1594b and venetoclax exerted significant synergy, resulting in enhanced differentiation and inhibited proliferation across several cell lines. In the *NPM1*-mutated AML PDX model, DS-1594b single-agent treatment significantly extended survival. Importantly, compared with DS-1594b monotherapy, the combination of DS-1594b and venetoclax more profoundly reduced leukemic burden and prolonged mouse survival. Menin inhibition was the primary driver of transcription changes in this model and impacted the expression of antiapoptotic regulators, providing a mechanistic explanation for the synergy observed between these drugs. Overall, we observed synergistic effects on differentiation induction and proliferation inhibition, both *in vitro* and *in vivo*. Together, our studies underscore the promise of this combination strategy as a novel therapeutic approach for improving treatment outcomes in patients with these specific genomic alterations.

INTRODUCTION

Acute leukemias are a heterogeneous group of aggressive blood cancers characterized by the rapid proliferation of immature white blood cells in the bone marrow. Among these, *MLL* (mixed-lineage leukemia, *KMT2A*) rearrangements and *NPM1* (nucleophosmin 1) mutations represent two distinct subtypes, each posing significant clinical challenges[1,2]. *MLL* rearrangements (*MLLr*) are a common genetic anomaly in pediatric hematologic malignancies, where they are found in up to 80% of infant acute lymphoblastic leukemia patients[3]. However, in adult acute myeloid leukemia (AML), they occur in only 5% to 10% of cases[4]. These rearrangements arise from translocations involving the MLL gene, producing fusion proteins that enhance proliferation, block differentiation, and drive aggressive leukemias[5]. Unfortunately, *MLL*-rearranged leukemias are notoriously resistant to conventional treatment approaches and associated with high early mortality, resulting in a distressingly low 5-year survival rate of only 35% in newly diagnosed, and <10% in relapsed/refractory (R/R) AML[6].

In contrast, NPM1 mutations are among the most common alterations in adult AML, present in ~30% of cases[7]. The *NPM1* gene encodes a nucleolar phosphoprotein involved in various cellular processes, including ribosome biogenesis and centrosome duplication. Mutations in *NPM1* cause aberrant cytoplasmic localization, disrupting normal functions and promoting leukemogenesis through *HOX* gene activation[8,9]. Although *NPM1*-mutated AML generally has a favorable prognosis in the absence of *FLT3-ITD* mutations[10] It remains a clinical challenge in relapse/refractory and elderly patients[11].

Menin, encoded by *MEN1*, is a scaffold protein essential for regulating gene expression through its interactions with chromatin-modifying complexes and plays a crucial role in various cellular processes[12]. It was initially identified as the product of the MEN1 gene, linked to *Multiple Endocrine Neoplasia type 1*, a hereditary tumor syndrome[13]. Several studies have revealed the

critical role of protein-protein interactions between menin, MLL, and MLL fusion proteins in the pathogenesis of *MLL*-rearranged leukemias[14,15]. Similarly, mutated NPM1 interacts with the MLL complex to regulate oncogenic signatures in *NPM1*-mutated AML [16,17] . Consequently, targeting the menin-MLL interaction with additional menin inhibitors has emerged as a promising therapeutic strategy in preclinical and clinical studies of both *MLLr* and *NPM1*-mutated AML[18]. Notably, the first menin inhibitor revumenib was recently approved by the FDA for the treatment of relapsed or refractory acute leukemia with KMT2A translocations, marking a significant milestone in the treatment of these challenging leukemias[19]. Resistance mechanisms to menin inhibitors can include the appearance of specific point mutations that abrogate drug binding, but emerging evidence suggests that different inhibitors may have unique effects on the various pathways through which resistance develops[20]. Therefore, expanding preclinical data across a range of structurally distinct menin inhibitors remains an important task to refine therapeutic approaches.

Here, we investigated the preclinical potential of the novel menin-MLL inhibitor DS-1594b[21], in combination with venetoclax, a selective inhibitor of the antiapoptotic BCL2 protein[22]. Venetoclax has shown promising activity in AML, making it an ideal partner for targeted therapies[23]. We and others have shown that acute lymphoblastic leukemia cells with the t(4;11) MLL translocation express high BCL2 levels and are highly sensitive to venetoclax, as the resulting MLL/AF4 fusion protein upregulates BCL2 via increased H3K79me2/3 at its locus[24].

Here, we hypothesized that targeting the menin-MLL interaction using DS-1594b in combination with venetoclax may promote cell differentiation and enhance lethality in acute leukemias, particularly in MLL-rearranged and NPM1-mutated AML. To test this hypothesis, we utilized both cell lines and patient samples harboring either MLL rearrangements or NPM1 mutations and a patient-derived xenograft (PDX) model of NPM1-mutated acute leukemia to assess the

synergistic effects of DS-1594b and venetoclax on leukemic cell viability, apoptosis induction, and differentiation potential.

By evaluating this drug combination preclinically, our study aims to provide insights into a targeted therapeutic strategy for acute leukemias with *NPM1* mutations and *MLL* rearrangements[25], potentially supporting new treatment options for these high-risk patients.

METHODS

Cell lines and patient samples

AML cell lines with MLL rearrangements (OCI-AML2, MOLM-13, MOLM-14, MV4-11, MOLM-13 ven-res), NPM1 mutations (OCI-AML3, IMS-M2), and without these alterations (U937, HL60) were obtained from DSMZ and the University of Perugia[26]. Cells and patient samples (2,000–150,000/well) were treated with DS-1594b (0–10 μM, 5–10 days; Daiichi Sankyo[21]) and/or venetoclax (0–500 nM, 5 days; LC Laboratories[22]), except MV4-11 cells, which were treated for 3 days due to their higher sensitivity. This study was approved by the Institutional Review Board of The University of Texas MD Anderson Cancer Center (protocol LAB-01-473), and conducted in accordance with the Declaration of Helsinki; written informed consent was obtained from all participants.

Proliferation, viability, apoptosis, and differentiation assays

Cell proliferation was measured by quantifying ATP using a CellTiter-Glo Luminescent Cell Viability Assay (Promega). The effect of each treatment on the number of viable cells and apoptotic cells was evaluated by Annexin V–DAPI assay with flow cytometry. To evaluate differentiation, cells were stained with CD14, CD15, CD11b, CD45, and CD33 antibodies (BD Biosciences) and analyzed with flow cytometry.

Western blotting

Immunoblotting was performed as detailed in Baran et al.[27](Supplementary Methods). The antibody panel used is summarized in Table S1.

BH3 profiling

BH3 profiling was conducted as previously reported[28]. (Supplementary methods).

AML xenograft mouse study

40 female NSG mice (8–10 weeks old; Jackson Laboratory, NOD.Cg-Prkdc^scid Il2rgtm1Wjl/SzJ) were inoculated via tail vein with 3×10 NPM1m PDX/luc/GFP cells in 100 µL. After leukemia engraftment was confirmed by bioluminescence, mice (n = 10/group) were randomized to vehicle, venetoclax, DS-1594b, or the combination. DS-1594b (50 mg/kg) was given orally for 4 weeks starting 12 days post-injection; venetoclax was given orally at 50 mg/kg for 2 weeks, then 100 mg/kg for 2 weeks of a 28-day cycle. Mice were weighed weekly and sacrificed at endpoint per IACUC guidelines. Spleen PDX cells were barcoded and stained with metal-conjugated antibodies for CyTOF[29] . Bioluminescence images were acquired every 7–10 days using the IVIS Lumina LT system.

RNA-Seq analysis

FastQ files were quality checked using FastQC[30] and the reads were trimmed using Trim Galore! With the parameter --2colour 20. The trimmed reads were then mapped to hg38 reference genome using STAR[31]. Gene expression was then quantified using featureCounts[32]. DESeq2[33] was used to carry out differential gene analysis. Batch correction was carried out using RUVSeq[34]. Gene ontology enrichment analysis using biological process terms was performed using ClusterProfiler[35].

RESULTS

DS-1594b alone promotes differentiation in *MLL*-rearranged and *NPM1*-mutated cell lines

We first evaluated the impact of DS-1594b on the viability of various cell lines with *MLL* rearrangements (MOLM-13, MOLM-14, MV4-11) and *NPM1* mutations (OCI-AML3, IMS-M2) after 7 days of treatment. Our findings indicated that low μM concentrations of DS-1594b significantly reduced proliferation in these cell lines, while having no effect on non-*MLL*r/non-*NPM1*-mutated U937 and HL60 cells (Fig. 1A). Given the frequency of venetoclax resistance in AML, we generated venetoclax-resistant (ven-res) AML cell lines to evaluate whether menin inhibition could provide an alternative therapeutic option. To this end, we exposed MOLM-13, OCI-AML2, and MV4-11 cells to increasing concentrations of ABT-199, starting at 10 nM and increasing to 1 μM (see supplementary methods). Notably, the ven-res MOLM-13 cell line, along with the other two ven-res cell lines, OCI-AML2 and MV4-11, all of which harbor *MLL* rearrangements, showed varying responses to DS-1594b. MOLM-13 ven-res was sensitive to the treatment, while OCI-AML2 and MV4-11 ven-res did not respond (Figs. 1A and S1A).

Given the known effects of menin inhibitors on inducing cell differentiation[36], we assessed whether DS-1594b alone induced differentiation in the tested AML cell lines by examining differentiation markers (CD11b, CD14, CD15) using flow cytometry. Our results revealed that OCI-AML3[37,38], OCI-AML2, MOLM-13 ven-res, and MOLM-14 cell lines began to show differentiation effects (CD11b positivity) after 5 days (Fig. 1B), with the effects becoming more evident after 10 days of treatment (Fig. S1B). Of note, the differentiation marker CD15, expressed by neutrophils, was found to be upregulated only in the MOLM-14 cell line, while CD14, expressed by monocytes, was present only when CD11b was expressed after 10 days (Figs. S1C and S1D). No differentiation was observed in non-*NPM1*/non-*MLL*r cell lines like U937 or HL60, even at higher doses of DS-1594. Moreover, DS-1594b treatment induced apoptosis in OCI-AML2, OCI-AML3, and MV4-11 cells after 7 days (Fig. 1C). Notably, apoptosis

was also observed in MOLM-13 and MOLM-13 ven-res cell lines after 10 days of treatment (Fig. S1E). Western blot analysis performed after 5-day treatment with DS-1594b showed a reduction in menin protein levels across all leukemia cell lines, accompanied by decreased BCL-2 expression in OCI-AML3 and OCI-AML2, and reduced levels of the cell-cycle inhibitor p27 specifically in OCI-AML2 cells (Fig. 1D). Interestingly, when treated with DS-1594b, MCL-1 was upregulated in OCI-AML3 but not in the other cell lines. In addition, CD11b upregulation was found in OCI-AML2 and OCI-AML3, consistent with results observed from flow cytometry analysis.

Next, using dynamic BH3 profiling, we tested whether menin inhibition enhanced cell dependency on the antiapoptotic BCL-2 family members for survival (see supplemental methods). MV4-11 cells were pre-treated with DS-1594b followed by exposure to different BH3 mimetic peptides, and the mitochondrial outer membrane permeabilization was measured by flow cytometric monitoring of cytochrome c release after 24 hours. We observed that in both cell lines, inhibition of menin increased cell priming to the pan-activator and sensitizer hBIM, hBID-Y, PUMA, and Bmf-Y peptides (Figs. S2A and S2B), and only OCI-AML3 cells were additionally primed to MCL-1 targeting mNoxaA and MS1 peptides. This pattern indicates that while in MV4-11 cells, DS-1594b enhanced cell dependency on BCL-2, in OCI-AML3 cells the drug additionally increased their dependence on the antiapoptotic MCL-1 for survival.

Overall, our results demonstrate that DS-1594b induces differentiation of AML cells, consistent with a similar effect reported for other menin inhibitors in the literature[39], as well as blocking cell proliferation. Additionally, we observed significant apoptosis induction after prolonged treatment (7–10 days) in several cell lines. Importantly, menin inhibition primed AML cells to become more dependent on BCL-2 for survival.

Co-treatment with DS-1594b and venetoclax exerts synergistic *in vitro* lethality in AML cells expressing *MLL* rearrangements or *NPM1* mutations

Our findings of increased survival BCL-2 dependency upon Menin inhibition led us to explore the possibility that targeting BCL-2 with clinically used venetoclax may enhance the anti-AML efficacy of DS-1594b in cells expressing *NPM1* mutant proteins or MLL fusion proteins.

To this end, we tested the efficacy of combined DS-1594b and venetoclax treatment in the same *MLL*-rearranged and *NPM1*-mutated cell lines described previously. These combination experiments were performed using a 5-day treatment schedule (except for MV4-11, treated for 3 days), which was selected to capture the full range of drug responses and potential synergistic effects, especially given the delayed activity typically observed with Menin inhibitors in AML. Combination treatment significantly reduced proliferation in all MLLr and NPM1-mutant lines, while sparing control lines (HL60, U937) (Fig. 2A). Notably, the MV4-11 cell line displayed significant inhibition after just 3 days of treatment (CI=0.07), suggesting heightened sensitivity to the drug combination, as did the MOLM-13 and MOLM-14 cell lines after 5 days of treatment (CI=0.25, CI=0.16 respectively). Moreover, the *NPM1*-mutated IMS-M2 cell line exhibited inhibition only when treated with the drug combination, not when treated with either drug alone (CI=0.005). In addition, Bliss synergy score analysis revealed synergy of the combined treatment in MOLM-14, but not in U937 cells (Fig. S2C), confirming efficacy of both drugs in *MLL*-rearranged AML cell lines.

Next, we analyzed the effects of co-treatment with venetoclax and DS-1594b on apoptosis using flow cytometry for Annexin-V and a Western blot assay. All tested cell lines, except the negative control U937, underwent apoptosis following combined treatment (Fig. S3A). Notably, in OCI-AML2 cells, the combination efficacy is primarily driven by venetoclax. Additionally, the Western blot analysis (Fig. 2B) demonstrated increased levels of PARP-C and decreased level of total Caspase-3, both well-known apoptosis hallmarks. CD11b was upregulated in OCI-AML3, and menin was downregulated in all cell lines. The expression of MCL-1 persisted in OCI-AML3 cells after treatment with the combination for 3 days, consistent with increased priming by BH3

profiling, yet was reduced after 5 days likely due to a change in cell state due to differentiation. In addition, P27 is downregulated in all cell lines except for the U937 cell line control. These outcomes were contrary to what was observed when DS-1594b was used alone.

These findings collectively confirm that DS-1594b and venetoclax combination treatment effectively inhibits proliferation and induces apoptosis in cell lines with *MLL* rearrangements and *NPM1* mutations, achieved through the activation of the PARP-c and caspase-3-c pathways.

DS-1594b and venetoclax combination therapy promotes differentiation and shows enhanced lethality in primary AML patient samples harboring *MLL* rearrangements or *NPM1* mutations

Next, we investigated the potential of a combination DS-1594b and venetoclax treatment to induce differentiation and lethality in primary samples from AML patients that harbor *MLL* rearrangements or *NPM1* mutations. Our findings provide evidence that the combined treatment exerted a moderate synergistic effect, in 4 out of 6 tested patient samples (Figs. 3A and S4A). Importantly, among these, 3 out of 5 patient samples with *MLL* rearrangement exhibited synergistic inhibition of viability as shown by Bliss synergy score, indicating a favorable response to menin/BCL-2 inhibition. Sample from patient 3 (PT3) however, displayed resistance to menin inhibition. Additionally, dual combination demonstrated a slight synergistic effect in patient sample PT6 with an *NPM1* mutation (Figs. 3A and S4A). In turn, DS-1594b alone led to a substantial increase in the differentiation of AML cells, particularly in PT2 and PT6 (Fig. 3B), and less so in other patient samples treated with DS-1594b alone.

Overall, our results suggest that the combination therapy of a menin inhibitor and venetoclax may be a promising treatment strategy for AML patients with *MLL* rearrangements or *NPM1*

mutations. Furthermore, our findings highlight the potential of using DS-1594b as a single agent to promote AML cell differentiation.

In vivo efficacy of the combination of DS-1594b with venetoclax in PDXs with *NPM1* mutations

After observing moderate synergy between DS-1594b and venetoclax against AML cells with *MLL* rearrangements or *NPM1* mutations *in vitro*, next we assessed anti-leukemia efficacy of dual combination *in vivo* using NSG mice engrafted with *NPM1*-mutated AML cells in a PDX luciferase-expressing model. We tested DS-1954b and venetoclax individually and in combination at well-tolerated doses. We found that co-treatment with DS-1594b and venetoclax for 4 weeks resulted in a greater reduction in AML burden compared with treatment with either single-agent treatment or the vehicle control. Bioluminescence imaging demonstrated the efficacy of the combination treatment (Figs. 4A and 4B). Importantly, the weight of the mice in the combination group was not significantly affected, indicating good tolerance, whereas venetoclax and control groups experienced significant weight reduction (Fig. 4C). Interestingly, there was no difference in weight between the DS-1594b and combination groups. Furthermore, the combination and single-agent DS-1594b group had a reduced spleen weight compared with the other groups indicative of a significant suppression of AML progression in the treated groups. (Figs. 4D and S5A). No differences were observed in bone marrow engraftment (Fig. S5B). The survival curve clearly demonstrated the benefits of the combination treatment, with the DS-1594b group showing some benefit but the combination group showing the greatest benefit (Fig. 4E). Notably, this PDX appeared resistant to Venetoclax, as demonstrated by the survival curve and bioluminescence images.

Next, we tested whether the addition of venetoclax further enhanced leukemia differentiation compared to menin inhibition alone. To this end, we performed high-dimensional mass cytometry (CyTOF) using a comprehensive panel of surface and intracellular markers to assess changes in protein expression across multiple pathways, with a particular focus on markers associated with myeloid and monocytic differentiation (Fig. 5A). This approach enabled a detailed phenotypic characterization of leukemic cells following *in vivo* treatment. For this analysis, cells from the PDX spleen were stained with anti-human antibodies against differentiation markers and leukemia markers (Table S2). We found that single agent DS-1594b as well as combined treatment led to the emergence of a population of cells (pop1) with elevated expression of CD33, CD13, and CD44, which are well-known markers of myeloid cell differentiation[40–42] (Figs. 5B-C and S5C). Importantly, this population of cells did not significantly increase in the combined treatment compared to DS-1594b alone, suggesting that the observed differentiation of AML cells was driven mainly by DS-1594b.

Menin inhibition potentiates venetoclax treatment via transcriptional mechanisms

To better understand the molecular mechanisms underlying the impact of the combined venetoclax/menin treatment, we performed RNA-seq on PDX spleen cells harboring *NPM1*c, DNMT3A and FLT3-ITD mutations[43] after 4 weeks of treatment *in vivo*. Comparing across single and combination treatments, it was apparent that most differences in gene expression were driven by the DS-1594b-mediated inhibition of menin, with few additional gene expression changes induced by the combined treatment (Fig. 6A). Classic menin targets, such as *MEIS1*, *FLT3* and *HOXA9*, had decreased expression (Fig. S5D). Cluster 1 and 4 genes (decreased expression in DS-1594b and Combination) were enriched for DNA replication, cell division, and RNA processing, whereas Cluster 5 genes (decreased expression with VEN and Combination) were enriched for interferon response and response to virus (Fig. S5E).

Interestingly, there was a small subset of genes that were further downregulated or upregulated in the combination treatment compared to menin inhibition alone (Fig. 6B, clusters 3 and 4). Based on this we hypothesized that menin inhibition might drive the downregulation of anti-apoptotic factors, which could be further potentiated by co-treatment with venetoclax. To explore this possibility, we focused on key anti-apoptotic genes and found that DS-1594b suppressed expression of MCL-1 (Fig. 6C). Importantly, this effect was significantly augmented by combined treatment with venetoclax. Given that upregulation of MCL-1 is a well-defined factor underlying AML resistance to venetoclax[44], such profound effect of treatment on MCL-1 level could account for the synergy of combined therapy observed in the tested PDX model.

We performed additional RNA-seq in the NPM1-mutant cell line OCI-AML3 and the MLL-AF4 cell line MV4-11 and similarly observed that Menin inhibition drives the majority of transcriptional changes both alone and in combination with venetoclax (Figs. S6A and S6B), including down-regulation of known menin targets (Figs. S6C and S6D) and specific anti-apoptotic genes. We found that OCI-AML3 cells (Fig. S6E) specifically down-regulated BCL2 in response to treatment with Menin inhibition and with the combination. MV4-11 cells (Fig. S6F) exhibit statistically significant down-regulation of BCL2 and BCL2L10 with Menin inhibitor and combination treatment, along with subtle (but not significant) decreases in BCL2L12 and MCL1. This suggests that the specific anti-apoptotic genes affected by Menin inhibition may depend on the AML context. ChIP-seq for Menin showed that Menin binds directly to some anti-apoptotic genes in both our PDX models, primary patient cells from an NPM1-mutant AML, and cell lines (Fig. S6G), MV4-11 data were obtained from publicly available GEO dataset GSE196036), suggesting that these genes are directly regulated by Menin binding.

Although Menin inhibition appears to drive the majority of transcriptional changes in the combination treatment, we nonetheless wanted to determine if any gene expression changes were driven specifically by venetoclax. To better clarify the differences between the individual

treatments with Menin, Venetoclax, and the combination, we compared differentially expressed genes in each pairwise comparison: Venetoclax vs vehicle, DS-1954b vs Vehicle, and Combination vs Vehicle (Fig. S7A). The largest overlap of differentially expressed genes was between down-regulated genes with Menin inhibition and combination treatment. Of the genes that are down-regulated with the combination but not Menin inhibition, only 5 genes are also down-regulated with Venetoclax alone, suggesting that the addition of venetoclax to DS-1954b induces these changes. In a pairwise comparison of vehicle vs venetoclax treated cells, there were 76 downregulated and 73 upregulated genes (Fig. 6D). A GO enrichment analysis of the genes downregulated in venetoclax-treated cells revealed that they were related to apoptosis, although it is likely that this regulation is indirect (Fig. 6E), given that venetoclax primarily functions as a BCL-2 inhibitor rather than directly influencing gene transcription.

These data indicate that venetoclax and menin inhibitors act through distinct mechanisms, with menin inhibition mainly impacting transcriptional programs, while synergy between the two agents occurs through modulation of anti-apoptotic pathways. Overall, our findings support the combination of DS-1594b and venetoclax as a promising therapeutic strategy with potent anti-leukemic activity in vivo for patients with *MLL* rearrangements and *NPM1* mutations.

DISCUSSION

In this study, we investigated the potential of combining the menin inhibitor DS-1594b with the BCL-2 antagonist venetoclax in AML. We assessed its ability to promote differentiation and enhance lethality in AML cell lines and primary patient samples harboring *MLL* rearrangements or *NPM1* mutations. Additionally, we assessed the *in vivo* efficacy of this combination therapy using a PDX mouse model. Overall, DS-1594b alone primarily inhibited growth and promoted differentiation both *in vitro* and *in vivo*. Moreover, when combined with venetoclax, it effectively induced apoptosis in AML cell lines and *NPM1*-mutated AML PDX mouse model, presenting a promising treatment approach for patients with acute leukemias. These results are consistent

with previous studies reporting synergistic anti-leukemic effects of venetoclax in combination with other menin inhibitors[45,46].

The decreased expression of menin and BCL-2 family members, along with the activation of apoptotic pathways, highlights a potential mechanism for the observed effects. Notably, the MV4-11 and MOLM-13 cell lines displayed heightened sensitivity to treatment with DS-1594b and venetoclax, emphasizing the therapeutic potential of this combination in AML subtypes with *FLT3-ITD* mutations.

Our investigation extended to primary AML patient samples harboring *MLL* rearrangements or *NPM1* mutations. Encouragingly, the combination treatment synergistically inhibited cell proliferation in most tested samples, particularly those with *MLL* rearrangements. These results underscore the potential clinical relevance of DS-1594b and venetoclax combination therapy. However, we also observed a lack of response in certain patient samples, indicating the need for further investigation into potential mechanisms of resistance and underscoring the importance of developing strategies to overcome resistance for more effective therapeutic outcomes in AML patients[47].

Our *in vivo* study using a PDX mouse model corroborated our *in vitro* findings, as mice who were treated with DS-1594b and venetoclax had a significantly reduced AML burden compared with those who were treated with single agents or vehicle control. Importantly, the combination therapy did not adversely affect mouse weight, suggesting that the regimen was well-tolerated.

RNA-seq analysis revealed that while most differences in gene expression were driven by the menin inhibitor, only a small subset of genes exhibited further modulation upon combination treatment. Specifically, we observed a significant downregulation of antiapoptotic MCL-1 in our PDX model and direct Menin binding at anti-apoptotic factor loci, including MCL1, suggesting an added complementary mechanism for the observed synergy between the two treatments.

Furthermore, our CyTOF analysis revealed increased expression of differentiation markers in the DS-1594b alone and combined treatment groups[48]. This finding supports that treatment with both DS-1594b and venetoclax may positively impact leukemic cell differentiation *in vivo*.

The observed synergistic effects on differentiation and apoptosis, *in vitro* and *in vivo*, have important clinical implications. However, while the study demonstrates efficacy in a subset of patient samples, the observed resistance in some cases underscores the AML clonal heterogeneity and complexity of finding universally effective treatments, in patients treated at the time of relapsed/refractory disease. These findings are particularly relevant in light of recent early-phase clinical trial data indicating promising activity of menin inhibitor/venetoclax combinations in the relapsed/refractory setting[49] and high response rates with a triple combination of azacitidine/venetoclax and Menin inhibitors in the R/R and older frontline AML patients[50]. Therefore, further studies are needed to explore the mechanistic underpinnings of this synergy and identify potential biomarkers of patient response and resistance. In conclusion, these results underscore the potential of DS-1594b and venetoclax as a targeted combination therapy, offering a promising and novel approach to specifically counteract the survival and differentiation blockades in AML patients with *MLL* rearrangements and *NPM1* mutations, and laying the groundwork for more personalized and effective treatment regimens in this patient population.

REFERENCES

1. Ley TJ, Miller C, Ding L, et al. Genomic and epigenomic landscapes of adult de novo acute myeloid leukemia. N Engl J Med. 2013;368(22):2059-2074.
2. Slany RK. The molecular biology of mixed lineage leukemia. Haematologica. 2009;94(7):984-993.
3. Andersson AK, Ma J, Wang J, et al. The landscape of somatic mutations in infant MLL-rearranged acute lymphoblastic leukemias. Nat Genet. 2015;47(4):330-337.
4. Britten O, Ragusa D, Tosi S, Kamel YM. MLL-Rearranged Acute Leukemia with t(4;11)(q21;q23)—Current Treatment Options. Is There a Role for CAR-T Cell Therapy? Cells. 2019;8(11):1341.
5. Daser A, Rabbitts TH. The versatile mixed lineage leukaemia gene MLL and its many associations in leukaemogenesis. Semin Cancer Biol. 2005;15(3):175-188.
6. Issa GC, Zarka J, Sasaki K, et al. Predictors of outcomes in adults with acute myeloid leukemia and KMT2A rearrangements. Blood Cancer J. 2021;11(9):162.
7. Falini B, Brunetti L, Sportoletti P, Paola Martelli M. NPM1-mutated acute myeloid leukemia: from bench to bedside. Blood. 2020;136(15):1707-1721.
8. Falini B, Mecucci C, Tiacci E, et al. Cytoplasmic nucleophosmin in acute myelogenous leukemia with a normal karyotype. N Engl J Med. 2005;352(3):254-266.
9. Brunetti L, Gundry MC, Sorcini D, et al. Mutant NPM1 Maintains the Leukemic State through HOX Expression. Cancer Cell. 2018;34(3):499-512.e9.
10. Döhner H, Wei AH, Appelbaum FR, et al. Diagnosis and management of AML in adults: 2022 recommendations from an international expert panel on behalf of the ELN. Blood. 2022;140(12):1345-1377.
11. Issa GC, Bidikian A, Venugopal S, et al. Clinical outcomes associated with NPM1 mutations in patients with relapsed or refractory AML. Blood Adv. 2023;7(6):933-942.
12. Matkar S, Thiel A, Hua X. Menin: a scaffold protein that controls gene expression and cell signaling. Trends Biochem Sci. 2013;38(8):394-402.
13. Carroll RW. Multiple endocrine neoplasia type 1 (MEN1). Asia Pac J Clin Oncol. 2013;9(4):297-309.
14. Grembecka J, He S, Shi A, et al. Menin-MLL inhibitors reverse oncogenic activity of MLL fusion proteins in leukemia. Nat Chem Biol. 2012;8(3):277-284.
15. Yokoyama A, Somervaille TCP, Smith KS, Rozenblatt-Rosen O, Meyerson M, Cleary ML. The menin tumor suppressor protein is an essential oncogenic cofactor for MLL-associated leukemogenesis. Cell. 2005;123(2):207-218.
16. Uckelmann HJ, Haarer EL, Takeda R, et al. Mutant NPM1 Directly Regulates Oncogenic Transcription in Acute Myeloid Leukemia. Cancer Discov. 2023;13(3):746-765.

17. Wang XQD, Fan D, Han Q, et al. Mutant NPM1 Hijacks Transcriptional Hubs to Maintain Pathogenic Gene Programs in Acute Myeloid Leukemia. Cancer Discov. 2023;13(3):724-745.

18. Issa GC, Aldoss I, DiPersio J, et al. The menin inhibitor revumenib in KMT2A-rearranged or NPM1-mutant leukaemia. Nature. 2023;615(7954):920-924.

19. Mullard A. FDA approves first menin inhibitor, for acute leukaemia. Nat Rev Drug Discov. 2025;24(1):7.

20. Bourgeois W, Cutler J, Rice HE, et al. Discerning the Landscape of Menin Inhibitor Resistance. Blood. 2024;144(Supplement 1):724.

21. Numata M, Haginoya N, Shiroishi M, et al. A novel Menin-MLL1 inhibitor, DS-1594a, prevents the progression of acute leukemia with rearranged MLL1 or mutated NPM1. Cancer Cell Int. 2023;23(1):36.

22. Pan R, Hogdal LJ, Benito JM, et al. Selective BCL-2 inhibition by ABT-199 causes on-target cell death in acute myeloid leukemia. Cancer Discov. 2014;4(3):362-675.

23. DiNardo CD, Pratz K, Pullarkat V, et al. Venetoclax combined with decitabine or azacitidine in treatment-naive, elderly patients with acute myeloid leukemia. Blood. 2019;133(1):7-17.

24. Benito JM, Godfrey L, Kojima K, et al. MLL-Rearranged Acute Lymphoblastic Leukemias Activate BCL-2 through H3K79 Methylation and Are Sensitive to the BCL-2-Specific Antagonist ABT-199. Cell Rep. 2015;13(12):2715-2727.

25. Wong NHM, So CWE. Novel therapeutic strategies for MLL-rearranged leukemias. Biochim Biophys Acta Gene Regul Mech. 2020;1863(9):194584.

26. Chi HT, Vu HA, Iwasaki R, et al. Detection of exon 12 type A mutation of NPM1 gene in IMS-M2 cell line. Leuk Res. 2010;34(2):261-262.

27. Baran N, Lodi A, Dhungana Y, et al. Inhibition of mitochondrial complex I reverses NOTCH1-driven metabolic reprogramming in T-cell acute lymphoblastic leukemia. Nat Commun. 2022;13(1):2801.

28. Vo TT, Ryan J, Carrasco R, et al. Relative mitochondrial priming of myeloblasts and normal HSCs determines chemotherapeutic success in AML. Cell. 2012;151(2):344-355.

29. Tan T, Gray DHD, Teh CE. Single-Cell Profiling of the Intrinsic Apoptotic Pathway by Mass Cytometry (CyTOF). Methods Mol Biol. 2022;2543:83-97.

30. Krueger F, James F, Ewels P, et al. FelixKrueger/TrimGalore: v0.6.10 - add default decompression path (0.6.10). Zenodo. Available at https://doi.org/10.5281/zenodo.7598955 Accessed on 2024, Feb 21.

31. Dobin A, Davis CA, Schlesinger F, et al. STAR: Ultrafast universal RNA-seq aligner. Bioinformatics. 2013;29(1):15-21.

32. Liao Y, Smyth GK, Shi W. FeatureCounts: An efficient general purpose program for assigning sequence reads to genomic features. Bioinformatics. 2014;30(7):923-930.

33. Love MI, Huber W, Anders S. Moderated estimation of fold change and dispersion for RNA-seq data with DESeq2. Genome Biol. 2014;15(12):550.

34. Risso D, Ngai J, Speed TP, Dudoit S. Normalization of RNA-seq data using factor analysis of control genes or samples. Nat Biotechnol. 2014 Sep;32(9):896-902.

35. Tianzhi W, Erqiang H, Shuangbin X, et al. clusterProfiler 4.0: A universal enrichment tool for interpreting omics data. Innovation (Camb). 2021;2(3):100141.

36. Swaminathan M, Bourgeois W, Armstrong SA, Wang ES. Menin Inhibitors in Acute Myeloid Leukemia-What Does the Future Hold? Cancer J. 2022;28(1):62-66.

37. Tiacci E, Spanhol-Rosseto A, Martelli MP, et al. The NPM1 wild-type OCI-AML2 and the NPM1-mutated OCI-AML3 cell lines carry DNMT3A mutations. Leukemia. 2012;26(3):554-557.

38. Quentmeier H, Martelli MP, Dirks WG, et al. Cell line OCI/AML3 bears exon-12 NPM gene mutation-A and cytoplasmic expression of nucleophosmin. Leukemia. 2005;19(10):1760-1767.

39. Fiskus W, Boettcher S, Daver N, et al. Effective Menin inhibitor-based combinations against AML with MLL rearrangement or NPM1 mutation (NPM1c). Blood Cancer J. 2022;12(1):5.

40. Schmits R, Filmus J, Gerwin N, et al. CD44 Regulates Hematopoietic Progenitor Distribution, Granuloma Formation, and Tumorigenicity. Blood. 1997;90(6):2217-2233.

41. Winnicka B, O'Conor C, Schacke W, et al. CD13 is dispensable for normal hematopoiesis and myeloid cell functions in the mouse. J Leukoc Biol. 2010;88(2):347.

42. Pei S, Pollyea DA, Gustafson A, et al. Monocytic subclones confer resistance to venetoclax-based therapy in patients with acute myeloid leukemia. Cancer Discov. 2020;10(4):536-551.

43. Pianigiani G, Gagliardi A, Mezzasoma F, et al. Prolonged XPO1 inhibition is essential for optimal antileukemic activity in NPM1-mutated AML. Blood Adv. 2022;6(22):5938-5949.

44. Choudhary GS, Al-Harbi S, Mazumder S, et al. MCL-1 and BCL-xL-dependent resistance to the BCL-2 inhibitor ABT-199 can be overcome by preventing PI3K/AKT/mTOR activation in lymphoid malignancies. Cell Death Dis. 2015;6(1):e1593.

45. Rausch J, Dzama MM, Dolgikh N, et al. Menin inhibitor ziftomenib (KO-539) synergizes with drugs targeting chromatin regulation or apoptosis and sensitizes acute myeloid leukemia with MLL rearrangement or NPM1 mutation to venetoclax. Haematologica. 2023;108(10):2837-2843.

46. Carter BZ, Tao W, Mak PY, et al. Menin inhibition decreases Bcl-2 and synergizes with venetoclax in NPM1/FLT3-mutated AML. Blood. 2021;138(17):1637-1641.

47. Perner F, Stein EM, Wenge D V, et al. MEN1 mutations mediate clinical resistance to menin inhibition. Nature. 2023;615(7954):913-919.

48. Krivtsov A V, Evans K, Gadrey JY, et al. A Menin-MLL Inhibitor Induces Specific Chromatin Changes and Eradicates Disease in Models of MLL-Rearranged Leukemia. Cancer Cell. 2019;36(6):660-673.e11.

49. Wei AH, Searle E, Aldoss I, et al. A PHASE 1B STUDY OF THE MENIN-KMT2A INHIBITOR JNJ-75276617 IN COMBINATION WITH VENETOCLAX AND AZACITIDINE IN RELAPSED/REFRACTORY ACUTE MYELOID LEUKEMIA WITH ALTERATIONS IN KMT2A OR NPM1. EHA Library. 2024;422237:S133.

50. Zeidner J, Lin TL, Welkie R, et al. PHASE 1B STUDY OF AZACITIDINE, VENETOCLAX AND REVUMENIB IN NEWLY DIAGNOSED OLDER ADULTS WITH NPM1 MUTATED OR KMT2A REARRANGED AML: INTERIM RESULTS OF DOSE ESCALATION FROM THE BEATAML CONSORTIUM. EHA Library. 2024;422238:S134.

FIGURE LEGENDS

Figure 1. DS-1594b alone promotes differentiation in *MLL*-rearranged and *NPM1*-mutant cell lines.

A. A proliferation assay was conducted by treating cell lines with *MLL* rearrangements (OCI-AML2, MOLM-13, MOLM-14, MV4-11, MOLM-13 ven-res) and *NPM1* mutations (OCI-AML3 and IMS-M2) and negative control cell lines (U937 and HL60) with DS-1594b alone at concentrations between 0.0001 µM and 9 µM for 7 days. Dose-response curves were analyzed using a curve-fitting routine based on nonlinear regression to compute the IC_{50} value. **B.** Apoptotic cells were identified by flow cytometry using counting beads, Annexin V, and DAPI after 7 days. Two-way ANOVA was performed to determine statistical significance (*, $P < 0.05$; **, $P < 0.01$; ***, $P < 0.001$; ****, $P < 0.0001$). **D.** OCI-AML3, HL60, OCI-AML2, and IMS-M2 cells were treated with the indicated concentrations of DS-1594b for 5 or 7 days. Following this, total cell lysates were prepared, and BCA protein assay was performed, and 30 µg of protein was loaded for western blot analyses. The expression levels of β-Actin in the lysates served as the loading control.

Figure 2. Co-treatment with DS-1594b and venetoclax exerts synergistic *in vitro* lethality in AML cells expressing *MLL* rearrangements or *NPM1* mutations.

A. Proliferation assay was conducted by treating cell lines with *MLL* rearrangements (OCI-AML2, MOLM-13, MOLM-14, MV4-11, MOLM-13 ven-res) and *NPM1* mutations (OCI-AML3 and IMS-M2) and negative control cell lines (U937 and HL60) with DS-1594b alone, venetoclax alone, or a combination treatment with the indicated concentrations in a fixed ratio for 5 days. MV4-11 was treated for 3 days. The combination index (CI), based on the Chou–Talalay method, was determined by CalcuSyn software (version 2.0). **B.** Apoptosis assay was conducted by treating cells lines for 5 days, except for MV4-11, which was treated for 3 days,

with the indicated concentrations. Apoptotic cells were determined by flow cytometry using counting beads, Annexin V, and DAPI. Two-way ANOVA was performed to determine statistical significance between DMSO and combo treatment (*, $P < 0.05$; **, $P < 0.01$; ***, $P < 0.001$; ****, $P < 0.0001$). DS= DS-1594b, Ven= Venetoclax. **C.** OCI-AML2, OCI-AML3, IMS-M2, MV4-11, and U937 cells were treated with the indicated concentrations of DS-1594b and venetoclax for 3 or 5 days. Following this, total cell lysates were prepared, BCA protein assay was performed, and 30 µg of proteins were loaded for western blot analyses. The expression levels of β-Actin in the lysates served as the loading control. DS= DS-1594b, Ven= Venetoclax.

Figure 3. Combination therapy promotes differentiation and shows enhanced lethality in primary AML patient samples harboring *MLL* rearrangements or *NPM1* mutations.

A. Patient cells with *MLL* rearrangements or *NPM1* mutations were treated with the indicated concentrations of DS-1594b and venetoclax for 3 days. Viable cell numbers were measured by quantifying ATP using a CellTiter-Glo Luminescent Cell Viability Assay. **B.** Four patients' cells were treated with vehicle (0.2 % DMSO) or 0.1 or 1 µM DS-1594b for 5 to 7 days. Differentiation effects were determined by flow cytometry using the CD11b marker. Single experiments were conducted due to the limited number of cells from the patients.

Figure 4. *In vivo* efficacy of the combination of DS-1594b with venetoclax in *NPM1*-mutated PDXs.

A. Bioluminescence imaging of tumor burden. Mice were inoculated via the tail vein with *NPM1*m PDX/luc/GFP; 3.0×106 cells/100 µL/mouse). Once leukemia engraftment was confirmed by bioluminescence imaging (day 0), mice (n = 10/group) were randomized to 4 treatment arms: vehicle; venetoclax alone, DS-1594b alone, and venetoclax/DS-1594b (combo). Bioluminescence imaging was performed at days 0, 10, 18, and 25 with IVIS Lumina LT *In Vivo* Imaging System. **B.** Total flux radiance of mice every 7 to 10 days from bioluminescence

imaging data. Two-way ANOVA was performed to determine significance (*, P < 0.05; **, P < 0.01; ***, P < 0.001; ****, P < 0.0001). **C.** Body weight was measured at days 10, 17, and 23. Two-way ANOVA was performed to determine statistical significance (*, P < 0.05; **, P < 0.01; ***, P < 0.001; ****, P < 0.0001). **D.** The spleen weight of three mice selected randomly from each treatment group was recorded. Two-way ANOVA was performed to determine statistical significance (*, P < 0.05; **, P < 0.01; ***, P < 0.001; ****, P < 0.0001). **E.** Kaplan–Meier survival curves of mice according to treatment arm (n = 10/group). Treatment started on day 12 and ended on day 40. Venetoclax (Ven) was administered at 50 mg/kg for 2 weeks followed by 100 mg/kg for 2 weeks; DS-1594b (DS) was given at 50 mg/kg for 4 weeks. Overall survival was estimated using the Kaplan–Meier method, and differences between groups were assessed using the Gehan–Breslow–Wilcoxon test (***, P < 0.001; ****, P < 0.0001).

Figure 5. DS-1594b drives differentiation in PDX model.

A. Human patient-derived xenograft (PDX) cells were collected from the spleens of three mice in each treatment group after 4 weeks of treatment. These cells were then stained for CyTOF analysis. Dimensionality reduction was performed using the t-distributed stochastic neighbor embedding method. Processed data were subjected to negative value pruned inverse hyperbolic sine transformation and clustered based on the PhenoGraph algorithm (k = 22) using all cell surface markers listed in Table S2. X= tSNE_1 Y=tSNE_2 **B.** Percentage of pop1 population events across the different group treatment. **C.** The expression levels of each protein within each population cluster. CD44, CD33, CD13 differentiation markers are highlighted

Figure 6. Menin inhibition potentiates venetoclax treatment via transcriptional mechanisms

A. Clustered heatmap of differentially expressed genes (p-adj < 0.05) in PDX-derived splenic leukaemia cells from mice treated for 4 weeks with vehicle control (Veh), venetoclax, Menin inhibitor (MENi) or a combination (Combo). **B.** Boxplots representing the patterns of expression (z-scored) of differentially expressed genes (p-adj < 0.05) from PDX-derived splenic leukaemia cells treated with vehicle control, venetoclax, Menin inhibitor, or a combination. **C.** Expression (CPM) of anti-apoptotic factors in PDX-derived splenic leukemia cells from mice treated with vehicle control, venetoclax, Menin inhibitor (MENi) or a combination. Statistical analysis was performed with an ANOVA followed by a Tukey test, where 1e-4 > `p-adj` < 1e-3 ~ "***", `p-adj` < 1e-2 ~ "**", `p-adj` < 5e-2 ~ "*", `p-adj` > 5e-2 ~ "NS". **D.** RNA-seq in PDX-derived splenic leukaemia cells from mice treated with venetoclax compared to vehicle control. Genes with the lowest adjusted p-value are labelled. **E.** GO:BP enrichment analysis of genes downregulated (p-adj < 0.05) with venetoclax treatment.

Figure 1

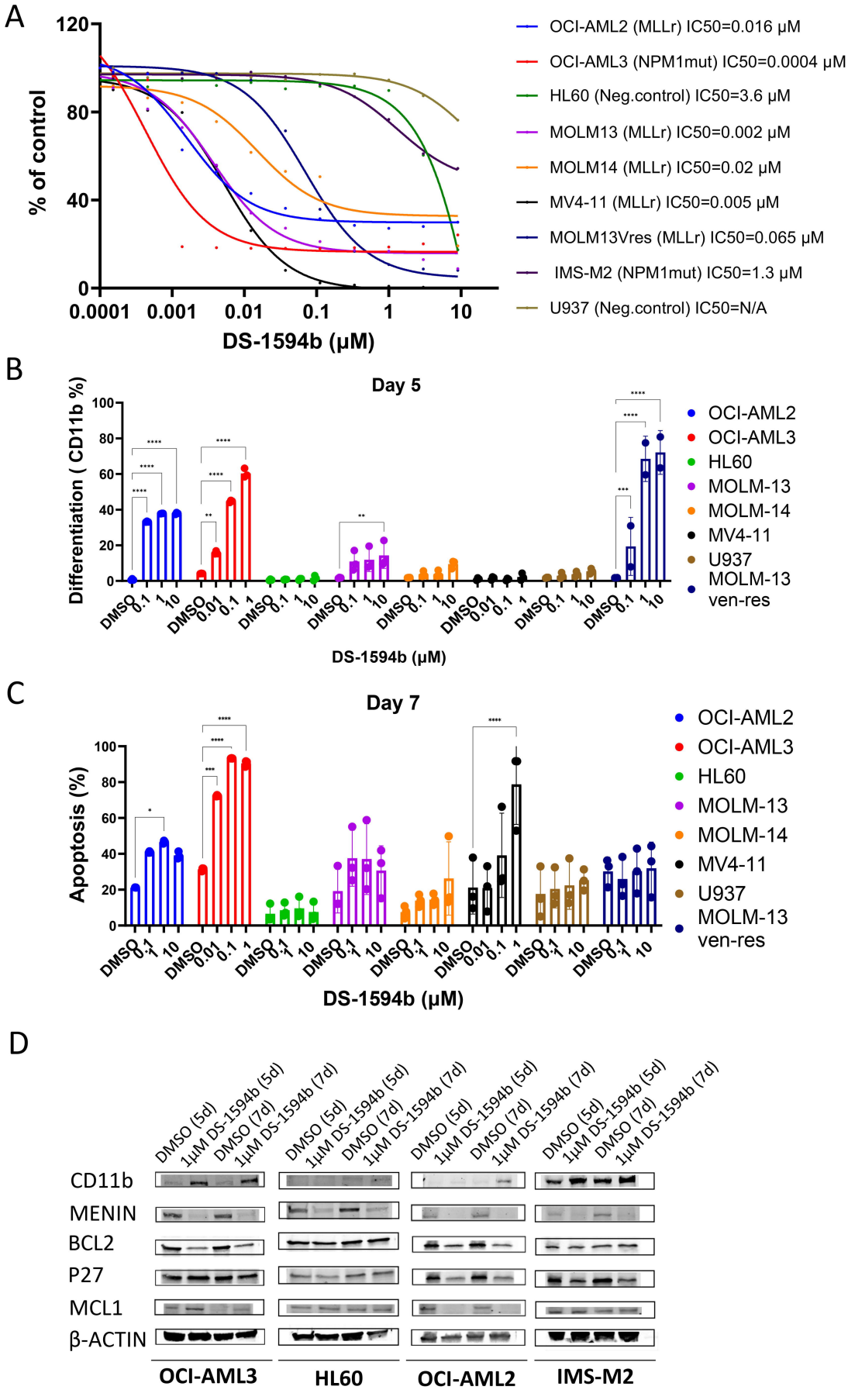
A
% of control
120
80
40
0
0.0001
0.001
0.01
0.1
1
10
DS-1594b (μM)
OCI-AML2 (MLLr) IC50=0.016 μM
OCI-AML3 (NPM1mut) IC50=0.0004 μM
HL60 (Neg.control) IC50=3.6 μM
MOLM13 (MLLr) IC50=0.002 μM
MOLM14 (MLLr) IC50=0.02 μM
MV4-11 (MLLr) IC50=0.005 μM
MOLM13Vres (MLLr) IC50=0.065 μM
IMS-M2 (NPM1mut) IC50=1.3 μM
U937 (Neg.control) IC50=N/A
B
Day 5
Differentiation (CD11b %)
DS-1594b (μM)
OCI-AML2
OCI-AML3
HL60
MOLM-13
MOLM-14
MV4-11
U937
MOLM-13 ven-res
C
Day 7
Apoptosis (%)
DS-1594b (μM)
OCI-AML2
OCI-AML3
HL60
MOLM-13
MOLM-14
MV4-11
U937
MOLM-13 ven-res
D
DMSO (5d)
1μM DS-1594b (5d)
DMSO (7d)
1μM DS-1594b (7d)
CD11b
MENIN
BCL2
P27
MCL1
β-ACTIN
OCI-AML3
HL60
OCI-AML2
IMS-M2

Figure 2

A

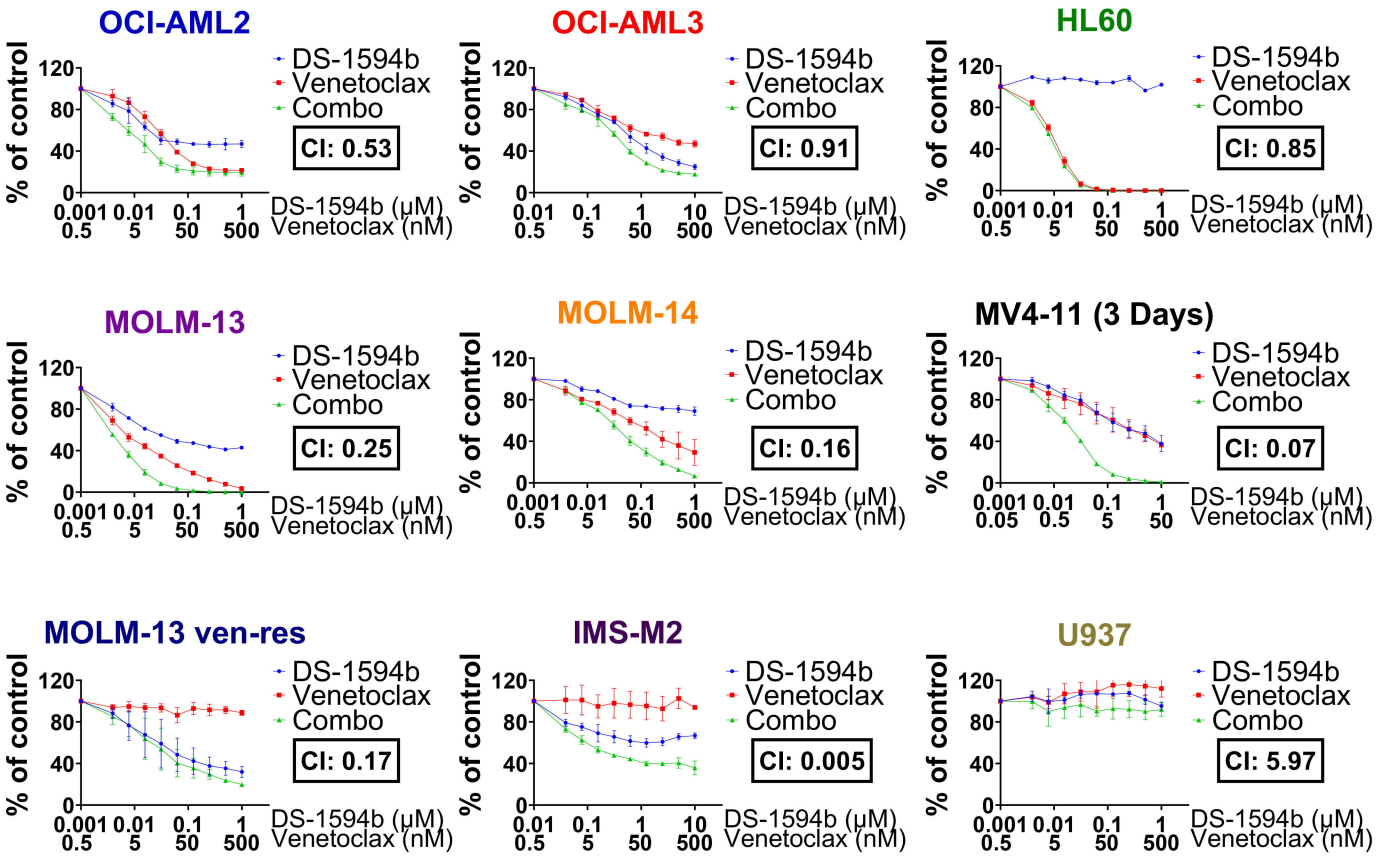
OCI-AML2
DS-1594b
Venetoclax
Combo
CI: 0.53
% of control
DS-1594b (μM)
Venetoclax (nM)
OCI-AML3
CI: 0.91
HL60
CI: 0.85
MOLM-13
CI: 0.25
MOLM-14
CI: 0.16
MV4-11 (3 Days)
CI: 0.07
MOLM-13 ven-res
CI: 0.17
IMS-M2
CI: 0.005
U937
CI: 5.97

B

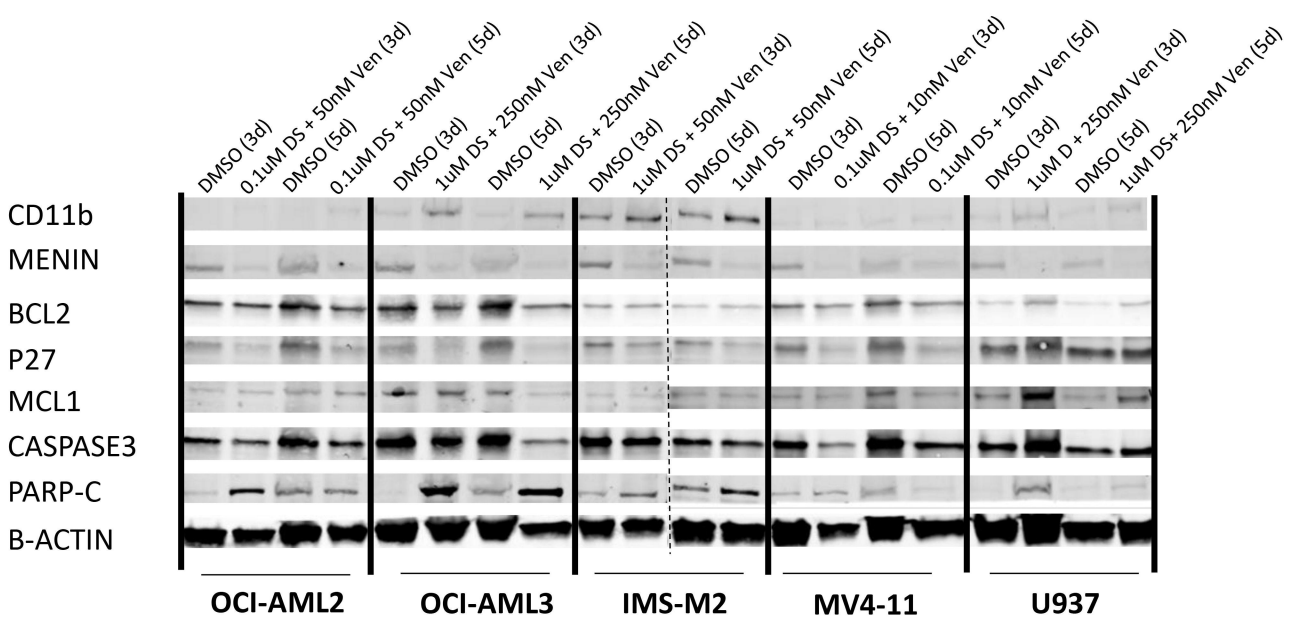
DMSO (3d)
0.1uM DS + 50nM Ven (3d)
DMSO (5d)
0.1uM DS + 50nM Ven (5d)
1uM DS + 250nM Ven (3d)
1uM DS + 250nM Ven (5d)
1uM DS + 50nM Ven (3d)
1uM DS + 50nM Ven (5d)
0.1uM DS + 10nM Ven (3d)
0.1uM DS + 10nM Ven (5d)
1uM D + 250nM Ven (3d)
1uM DS+ 250nM Ven (5d)
CD11b
MENIN
BCL2
P27
MCL1
CASPASE3
PARP-C
B-ACTIN
OCI-AML2
OCI-AML3
IMS-M2
MV4-11
U937

Figure 3

A

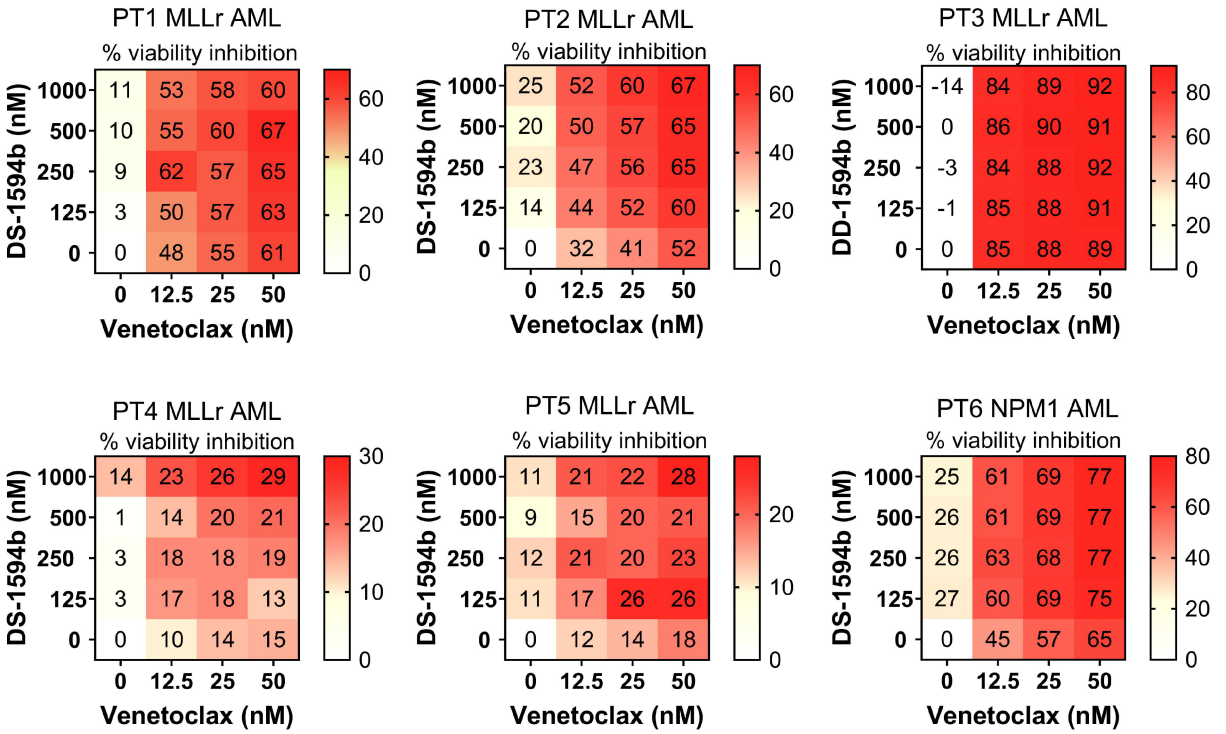
PT1 MLLr AML
% viability inhibition
DS-1594b (nM)
1000 11 53 58 60
500 10 55 60 67
250 9 62 57 65
125 3 50 57 63
0 0 48 55 61
0 12.5 25 50
Venetoclax (nM)
60 40 20 0
PT2 MLLr AML
% viability inhibition
DS-1594b (nM)
1000 25 52 60 67
500 20 50 57 65
250 23 47 56 65
125 14 44 52 60
0 0 32 41 52
0 12.5 25 50
Venetoclax (nM)
60 40 20 0
PT3 MLLr AML
% viability inhibition
DD-1594b (nM)
1000 -14 84 89 92
500 0 86 90 91
250 -3 84 88 92
125 -1 85 88 91
0 0 85 88 89
0 12.5 25 50
Venetoclax (nM)
80 60 40 20 0
PT4 MLLr AML
% viability inhibition
DS-1594b (nM)
1000 14 23 26 29
500 1 14 20 21
250 3 18 18 19
125 3 17 18 13
0 0 10 14 15
0 12.5 25 50
Venetoclax (nM)
30 20 10 0
PT5 MLLr AML
% viability inhibition
DS-1594b (nM)
1000 11 21 22 28
500 9 15 20 21
250 12 21 20 23
125 11 17 26 26
0 0 12 14 18
0 12.5 25 50
Venetoclax (nM)
20 10 0
PT6 NPM1 AML
% viability inhibition
DS-1594b (nM)
1000 25 61 69 77
500 26 61 69 77
250 26 63 68 77
125 27 60 69 75
0 0 45 57 65
0 12.5 25 50
Venetoclax (nM)
80 60 40 20 0

B

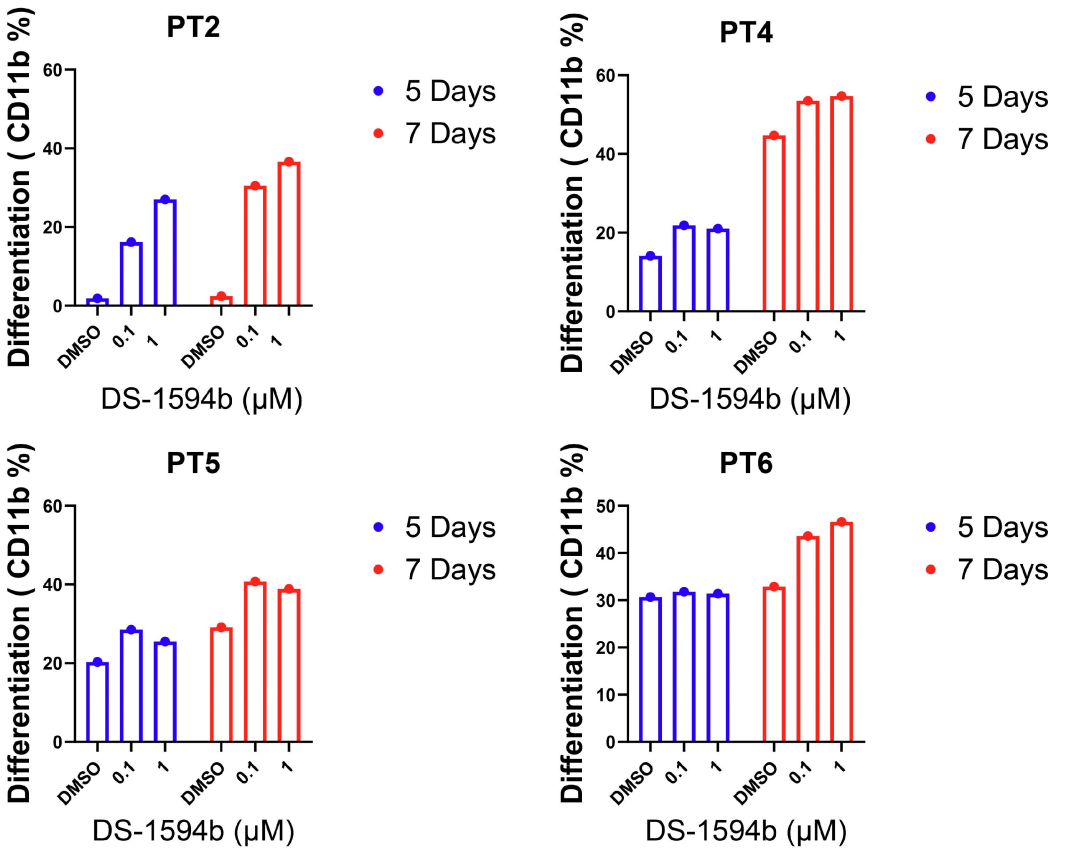
PT2
Differentiation (CD11b %)
60 40 20 0
DMSO 0.1 1 DMSO 0.1 1
DS-1594b (μM)
5 Days
7 Days
PT4
Differentiation (CD11b %)
60 40 20 0
DMSO 0.1 1 DMSO 0.1 1
DS-1594b (μM)
5 Days
7 Days
PT5
Differentiation (CD11b %)
60 40 20 0
DMSO 0.1 1 DMSO 0.1 1
DS-1594b (μM)
5 Days
7 Days
PT6
Differentiation (CD11b %)
50 40 30 20 10 0
DMSO 0.1 1 DMSO 0.1 1
DS-1594b (μM)
5 Days
7 Days

Figure 4

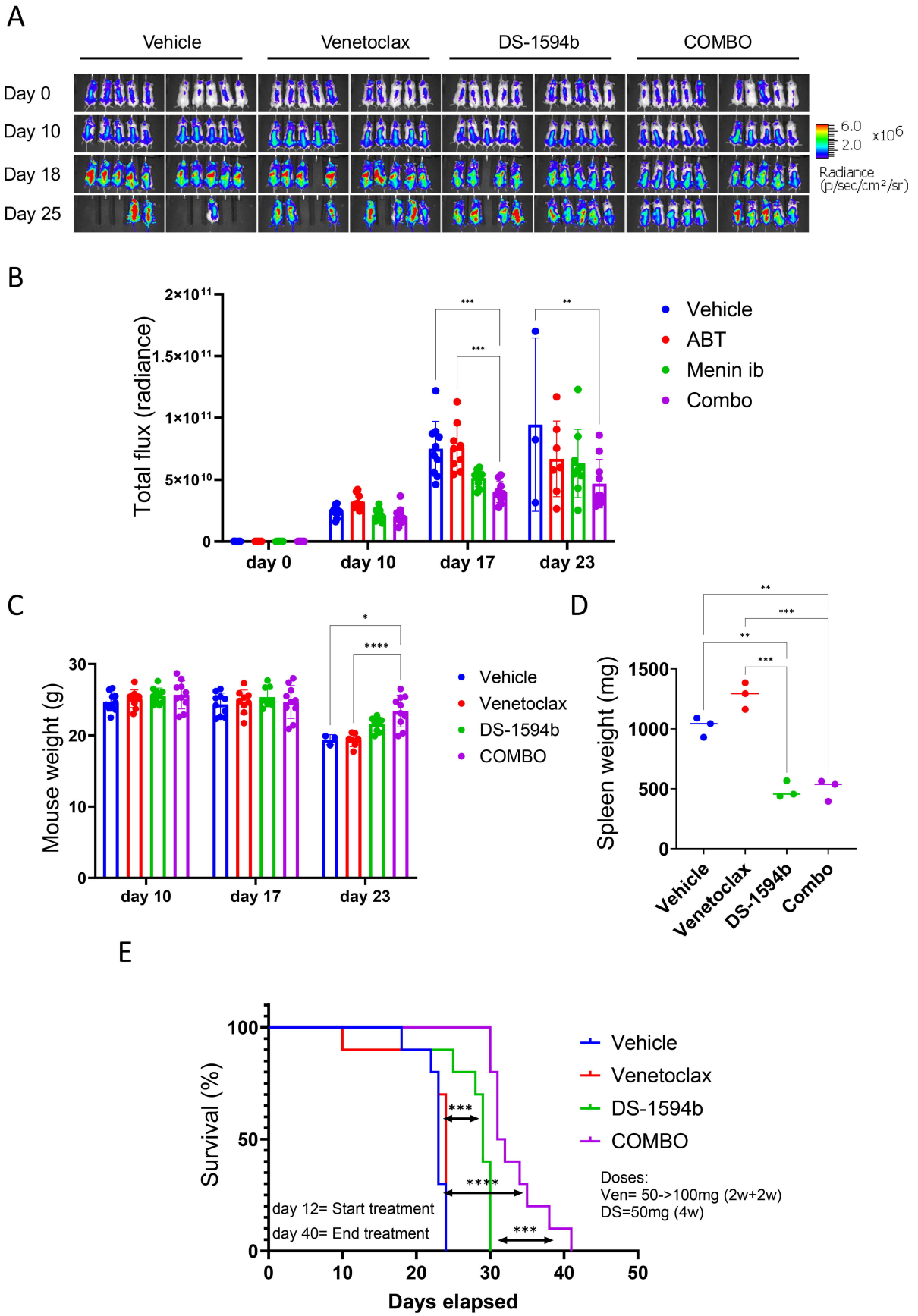
A
Vehicle
Venetoclax
DS-1594b
COMBO
Day 0
Day 10
Day 18
Day 25
6.0
2.0
x10^6
Radiance (p/sec/cm²/sr)
B
Total flux (radiance)
2×10^11
1.5×10^11
1×10^11
5×10^10
0
day 0
day 10
day 17
day 23
***
***
**
Vehicle
ABT
Menin ib
Combo
C
Mouse weight (g)
30
20
10
0
day 10
day 17
day 23
*
****
Vehicle
Venetoclax
DS-1594b
COMBO
D
Spleen weight (mg)
1500
1000
500
0
**
***
**
***
Vehicle
Venetoclax
DS-1594b
Combo
E
Survival (%)
100
50
0
0
10
20
30
40
50
Days elapsed
***
****
***
day 12= Start treatment
day 40= End treatment
Vehicle
Venetoclax
DS-1594b
COMBO
Doses:
Ven= 50->100mg (2w+2w)
DS=50mg (4w)

Figure 5

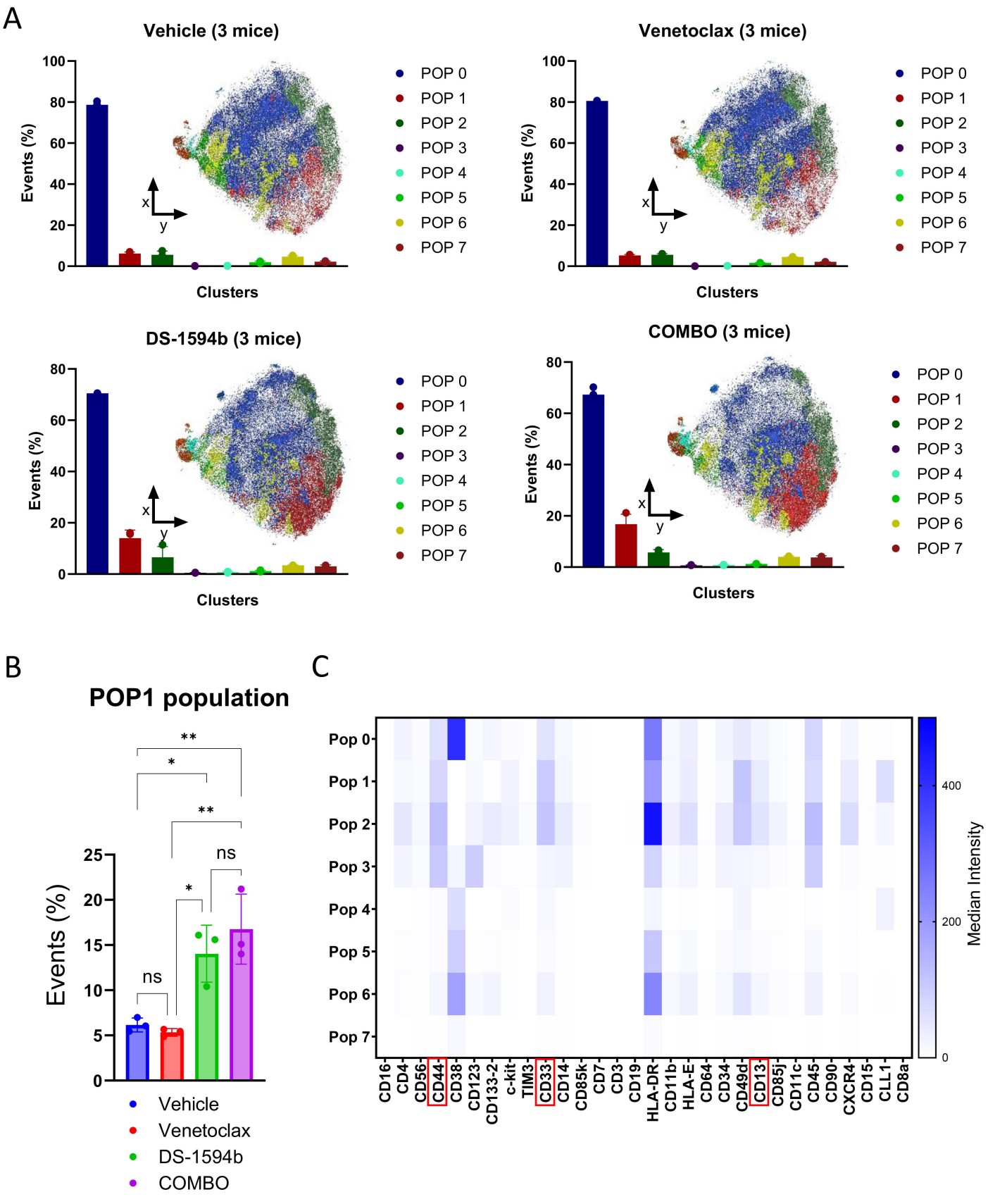
A
Vehicle (3 mice)
Venetoclax (3 mice)
DS-1594b (3 mice)
COMBO (3 mice)
Events (%)
Clusters
POP 0
POP 1
POP 2
POP 3
POP 4
POP 5
POP 6
POP 7
B
POP1 population
Events (%)
ns
*
**
Vehicle
Venetoclax
DS-1594b
COMBO
C
Pop 0
Pop 1
Pop 2
Pop 3
Pop 4
Pop 5
Pop 6
Pop 7
CD16
CD4
CD56
CD44
CD38
CD123
CD133-2
c-kit
TIM3
CD33
CD14
CD85k
CD7
CD3
CD19
HLA-DR
CD11b
HLA-E
CD64
CD34
CD49d
CD13
CD85j
CD11c
CD45
CD90
CXCR4
CD15
CLL1
CD8a
Median Intensity

Figure 6

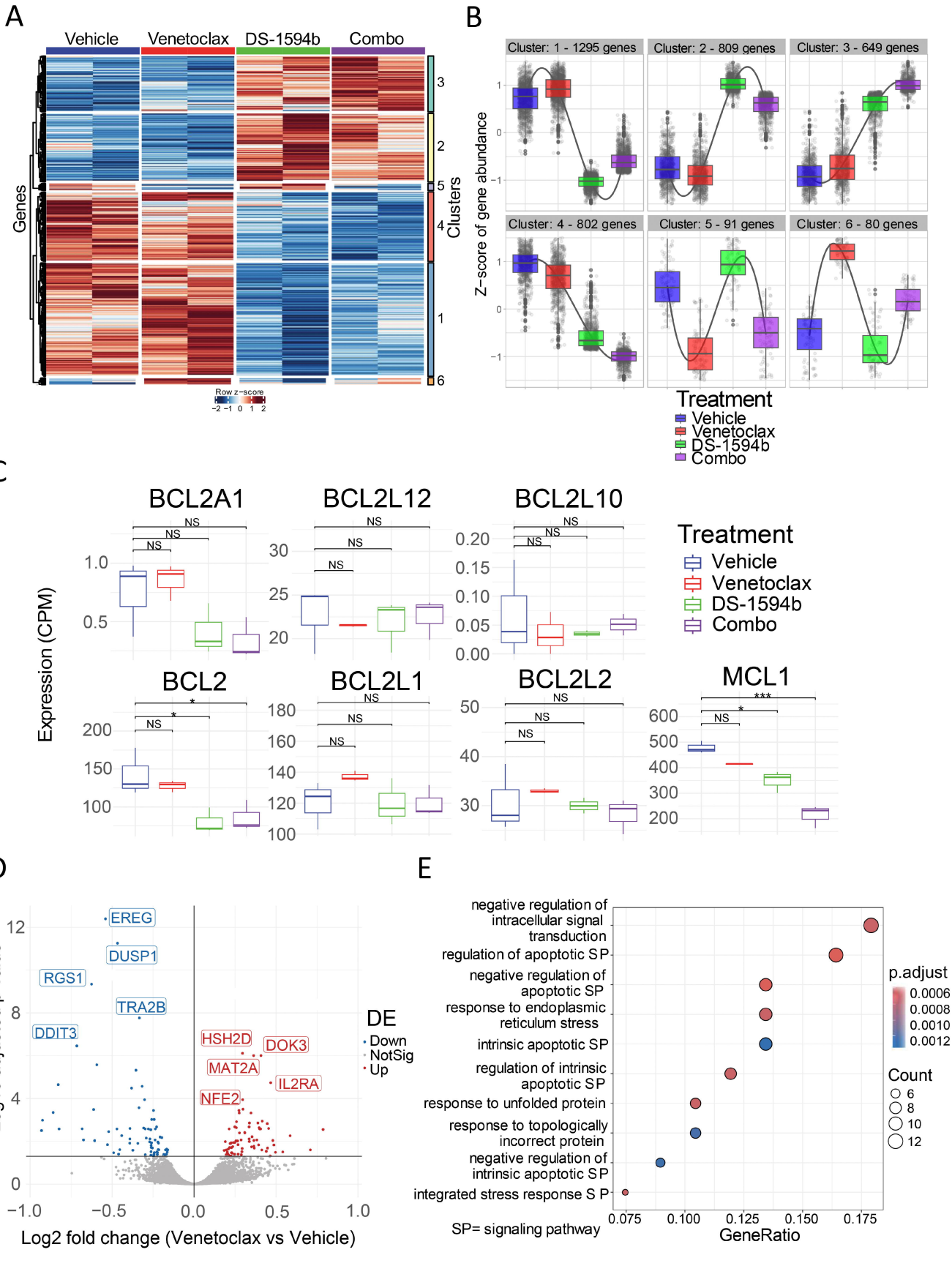
A
Vehicle
Venetoclax
DS-1594b
Combo
Genes
Clusters
Row z−score
B
Cluster: 1 - 1295 genes
Cluster: 2 - 809 genes
Cluster: 3 - 649 genes
Cluster: 4 - 802 genes
Cluster: 5 - 91 genes
Cluster: 6 - 80 genes
Z−score of gene abundance
Treatment
Vehicle
Venetoclax
DS-1594b
Combo
C
BCL2A1
BCL2L12
BCL2L10
BCL2
BCL2L1
BCL2L2
MCL1
Expression (CPM)
NS
*
***
D
EREG
DUSP1
RGS1
TRA2B
DDIT3
HSH2D
DOK3
MAT2A
IL2RA
NFE2
-Log10 adjusted p-value
Log2 fold change (Venetoclax vs Vehicle)
DE
Down
NotSig
Up
E
negative regulation of intracellular signal transduction
regulation of apoptotic SP
negative regulation of apoptotic SP
response to endoplasmic reticulum stress
intrinsic apoptotic SP
regulation of intrinsic apoptotic SP
response to unfolded protein
response to topologically incorrect protein
negative regulation of intrinsic apoptotic SP
integrated stress response S P
SP= signaling pathway
GeneRatio
p.adjust
Count

SUPPLEMENTARY METHODS

Cell lines and patient samples

AML cell lines OCI-AML2, OCI-AML3, HL60, MOLM-13, MOLM-14, MV4-11, MOLM-13 ven-res, and U937 were purchased from Deutsche Sammlung von Mikroorganismen und Zellkulturen. All cells were authenticated by short tandem repeat DNA fingerprinting in September 2016 by the Cytogenetics and Cell Authentication Core Facility at The University of Texas MD Anderson Cancer Center. IMS-M2 and NPM1 luc PDX were received from the University of Perugia under MTA agreement 25854. Primary AML patient bone marrow or peripheral blood samples (n = 6) were collected under MD Anderson IRB protocol LAB-01-473. All cell lines were cultured in suspension in RPMI-1640 medium (Sigma) and supplemented with 10% fetal bovine serum (Sigma), L-glutamine, and penicillin/streptomycin (Invitrogen).

Fresh whole blood samples from patients were mixed 1:1 with phosphate-buffered saline (PBS) without calcium and magnesium and added to 15 mL Lymphocyte Separation Medium (Sigma). Cells were centrifuged (1800 rpm for 20 min), and the mononuclear cell layer was extracted. Ammonium chloride solution (5 mL) was used to lyse residual red blood cells for 5 minutes while shaking. Primary AML patient cells were plated at 0.2-1.5 x 10^5 cells/mL in Stemline II (Milliporesigma), SCF (100 ng), FLT3L (100 ng), TPO (100 ng), IL3 (20 ng), and IL6 (20 ng) (Peptrotech).

Reagents

Venetoclax was purchased from LC Laboratories; DS-1594b was received from Daiichi SankyoCo., Ltd.; stock solutions for in vitro studies were prepared with DMSO (Sigma-Aldrich). For animal studies, DS-1594b was prepared in 0.1% methylcellulose and venetoclax was prepared in 10% ethanol/30% phosphal 50/60% PEG 400. Western blot antibodies were purchased from Cell Signaling (Table S1).

Generation of ven-res cell lines

OCI-AML2, MV4-11 and MOLM-13 AML cell lines were cultured in suspension in RPMI-1640 medium and supplemented with 10% fetal bovine serum, L-glutamine, and penicillin/streptomycin. Venetoclax resistance was induced by continuously exposing the parental cells to increasing concentrations of Venetoclax, starting at 10 nM and increasing to 1 μM. The medium with venetoclax was changed every 2 days. After cells achieved stable viability (above 90%) at a certain venetoclax dose, the dose was increased until it reached 1 μM.

Western Blotting

Cells (approximately 1-2 million per well) were plated in 6-well dishes. After undergoing treatment for the specified period, we extracted total proteins using Laemmli buffer and performed a Bicinchoninic acid assay (BCA). About 30 micrograms of these proteins were separated through sodium dodecyl sulfate-polyacrylamide gel electrophoresis and then transferred to polyvinylidene fluoride membranes provided by Millipore Sigma. Post-blocking with Li-COR Odyssey blocking buffer, these membranes were left to incubate with primary antibodies overnight at 4°C. Following this, they were washed and incubated for 2 hours with suitable infrared fluorochrome-conjugated secondary antibodies - Odyssey Irdye 680 RD anti-mouse and Odyssey Irdye 800 CW goat anti-rabbit. The protein signals were made visible using a LI-COR Odyssey imaging system.

BH3 profiling

BH3 profiling relies on the exposure of mitochondrial BCL-2 family of proteins to peptides that mimic endogenous pro-apoptotic BH3 activators and sensitizers that selectively bind to antiapoptotic BCL-2 family members. The release of cytochrome c from mitochondria in response to a given BH3 peptide therefore allows us to estimate the level of mitochondrial apoptotic priming (susceptibility of cells to commit apoptosis) and dependence on selective BCL-2 family members for survival. Cells were pelleted at 400 g and resuspended in DTEB (Derived from Trehalose

Experimental Buffer). Cells were permeabilized with digitonin and exposed to BH3 peptides (hBIM, PUMA, hBID-Y, Bmf-Y, mNoxaA, MS1; New England Peptide). The mitochondrial outer membrane permeabilization was monitored by cytochrome C release. Dimethyl sulfoxide (DMSO) and Ala were used as the negative and positive controls, respectively.

RNA sequencing

RNA was extracted from ~ 5 million cells using the Qiagen RNeasy Kit for RNA (74104) purification following the manufacturer's instructions. mRNA was purified using the NEBNext Poly(A) mRNA Magnetic Isolation Module (E7490S) using 1 µg of input RNA. Library preparation for sequencing was done using the NEBNext Ultra II Directional RNA Library Prep Kit for Illumina (E7760S). Samples were sequenced by paired-end sequencing on NextSeq500.

CyTOF protocol

Antibodies for time-of-flight mass cytometry (CyTOF) were either purchased from Fluidigm or conjugated in house as follows. Purified, carrier-free antibodies were conjugated with lanthanide isotopes using a MaxPar Antibody Labeling Kit (Fluidigm) following the manufacturer's instructions. Protein concentrations were determined using a NanoDrop 2000 spectrophotometer (Thermo Fisher Scientific), and metal contents of the conjugated antibodies were determined by CyTOF using a CyTOF mass cytometer (Fluidigm) in solution mode using Claritas PPT Grade Multi-Element Solution 1 (SPEX CertiPrep) with 0.5 ppb as a standard. Table S1 lists the antibodies used. All antibodies were labeled with heavy metals using Maxpar-X8 labeling reagent kits (Fluidigm) according to the manufacturer's instructions and titrated to determine the optimal concentration.

For each sample evaluated, 3×10^6 cells were aliquoted into separate fluorescence-activated cell sorting tubes and washed twice with Maxpar PBS buffer (Fluidigm; cat. 201058). For live/dead cell discrimination, cells were resuspended in 200 µL of 5 µM cisplatin (Fluidigm; cat. 201064) for

5 minutes on an orbital shaker, followed immediately by 3 washes in Maxpar cell staining buffer (CSB; Fluidigm; cat. 201068). Cells were then fixated for 10 minutes in 1 mL of 1× Fix I buffer (Fluidigm; cat. 201065), followed by 2 washes with 1× barcode perm buffer (Fluidigm; cat. 201057). Each unique palladium barcode (Fluidigm; Cell-ID 20-Plex Pd Barcoding Kit, cat. 201060) was suspended in 100 µL of barcode perm buffer and immediately transferred to cells in 800 µL of barcode perm buffer. Cells were incubated with barcodes for 30 minutes, then washed twice with 2 mL CSB. Barcoded cells were then combined into a single tube for CyTOF staining. The staining factor was calculated as the total number of barcoded cells/3 × 106 cells. Cells were blocked with 5 µL× staining factor of anti-human Fc receptor binding inhibitor (eBioscience Invitrogen) in 45 µL × staining factor of CSB for 15 minutes at room temperature. An appropriate amount of surface antibody master mix was added directly to the tube and incubated for 1 hour at room temperature before it was washed with CSB twice.

Next, cells were washed twice with PBS and stained for 30 minutes with antibodies against intracellular markers in a final reaction volume of 50 µL, washed twice with wash buffer and once with PBS, and stained for 20 minutes in 500 µL of 1:1000 iridium intercalator (Fluidigm; cat. 201192A) diluted in 1.6% PFA in PBS. Cells were then washed twice with wash buffer and filtered through blue-capped tubes. Each sample pellet was resuspended in 50 µL deionized water and transferred to a 96–deep-well plate containing 50 µL Eu151/153 calibration beads (Cat. 201073, Fluidigm). Samples were analyzed on a CyTOF mass cytometer using an AS5 Autosampler (Fluidigm); 0.4 mL deionized water was added to each sample just before injection. The data were saved in FCS3.0 format, de-barcoded by a Fluidigm de-barcoder, and analyzed by spanning-tree progression analysis of density-normalized events (SPADE) software (version 3) or Cytofkit for Bioconductor.

Data were initially filtered with FlowJo to eliminate normalization beads, debris, doublets, and non-viable cells. Subsequently, dimensionality reduction was conducted using the t-distributed

stochastic neighbor embedding technique. Processed information underwent a transformation using the negative value pruned inverse hyperbolic sine method and was then clustered employing the PhenoGraph algorithm (with a parameter k set to 22), utilizing the cell surface markers detailed in Table S2.

Statistical analyses

In vitro experiments were conducted in technical triplicate. The combination index (CI), based on the Chou–Talalay method (CalcuSyn version 2.0), was obtained at the effective doses of 50%, 75%, and 90% in the population exposed to the different agents (CI < 1, synergistic; CI = 1 additive; CI > 1, antagonistic). Bliss Synergy scores of the drugs combination treatment on cell lines were determined using Combenefit software. Statistical differences between groups were determined using a Student t-test or 2-way ANOVA with the Dunnett test. P less than or equal to 0.05 was considered statistically significant. Overall survival rate was estimated by the Kaplan–Meier method and compared using the log-rank test. Dose-response curves were analyzed using a curve-fitting routine based on nonlinear regression. All preceding analyses were performed utilizing GraphPad Prism 9 software.

Table S1.

Company	Cat. Number	Antibody
Cell Signaling	6891S	Menin (D45B1) XP® Rabbit mAb
Cell Signaling	49420S	CD11b/ITGAM (D6X1N) Rabbit mAb
Cell Signaling	3700S	β-Actin (8H10D10) Mouse mAb
Cell Signaling	9662S	Caspase-3 Antibody
Cell Signaling	9664S	Cleaved Caspase-3 (Asp175) (5A1E) Rabbit mAb
Cell Signaling	3686S	p27 Kip1 (D69C12) XP® Rabbit mAb
Cell Signaling	15071S	Bcl-2 (124) Mouse mAb
Cell Signaling	5625S	Cleaved PARP (Asp214) (D64E10) XP® Rabbit mAb
Cell Signaling	94296S	Mcl-1 (D2W9E) Rabbit mAb #

Table S2.

ID	Tagged Abs	Target	Label	Intracellular Staining	Clone	Specificities	Source	Cat
1	CD11c 159Tb	CD11c	159Tb	FALSE	Bu15	Hu	DVS-Fluidigm	3159001B
6	CD19 142Nd	CD19	142Nd	FALSE	HIB19	Hu	DVS-Fluidigm	3142001B
9	CD33 158Gd	CD33	158Gd	FALSE	WM53	Hu	DVS-Fluidigm	3158001B
11	CD11b 144Nd	CD11b	144Nd	FALSE	ICRF44	Hu	DVS-Fluidigm	3144001B
14	CD34 148Nd	CD34	148Nd	FALSE	581	Hu	DVS-Fluidigm	3148001B
17	CD44 166Er	CD44	166Er	FALSE	BJ18	Hu	DVS-Fluidigm	3166001B
41	CD90 171Yb	CD90	171Yb	FALSE	5.00E+10	Hu	BioLegend	328102
43	CXCR4 172Yb	CD184, CXCR4	172Yb	FALSE	12G5	Hu	BioLegend	306502
125	CD133/2 153Eu	CD133/2	153Eu	FALSE	293C3	Hu	Miltenyi	130-090-851
145	CD13 152Sm	CD13	152Sm	FALSE	WM15	Hu	DVS-Fluidigm	3152003B
175	HLA-E 145Nd	HLA-E	145Nd	FALSE	3D12	Hu	BioLegend	342602
183	CD49d 141Pr	CD49d	141Pr	FALSE	9F10	Hu	DVS-Fluidigm	3141004B
257	CD3 175Lu	CD3	175Lu	FALSE	UCHT1	Hu	BioLegend	300443
309	CD14 160Gd (MDA)	CD14	160Gd	FALSE	M5E2	Hu	BioLegend	301802
356	CD8a 176Yb	CD8a	176Yb	FALSE	HIT8a	Hu, Ch	BioLegend	300902
375	CD15 173Yb	CD15	173Yb	FALSE	W6D3	Hu	BioLegend	323002
394	CD64 146Nd	CD64	146Nd	FALSE	10.1	Hu	DVS-Fluidigm	3146006B
416	TIM-3 156Gd	TIM-3	156Gd	FALSE	F38-2E2	Hu, Rh	BioLegend	345002
455	CD4 161Dy	CD4	161Dy	FALSE	RPA-T4	Hu, Ch	BioLegend	300502
459	CD45 89Y	CD45	89Y	FALSE	HI30	Hu, Ch	DVS-Fluidigm	3089003B
467	CD56 163Dy	CD56	163Dy	FALSE	NCAM16.2	Hu	DVS-Fluidigm	3163007B
536	CD123 151Eu	CD123	151Eu	FALSE	7G3	Hu	BD	554527
538	CD38 167Er (MDA)	CD38	167Er	FALSE	HIT2	Hu	BioLegend	303502
557	Ki67 168Er	Ki67	168Er	TRUE	B56	Ms, Hu	BD	556003
558	CD85j 154Sm	CD85j, ILT2, LILRB1	154Sm	FALSE	HP-F1	Hu	BC	A07408
647	CD117 155Gd	CD117(c-kit)	155Gd	FALSE	104D2	Hu	BioLegend	313202
698	CD16 209Bi	CD16	209Bi	FALSE	3G8	Hu, Rh	DVS-Fluidigm	3209002B
824	CLL-1 174Yb (BL)	CD371, CLL-1, CLEC12A	174Yb	FALSE	50C1	Hu	BioLegend	353602
937	CD7 115In	CD7	115In	FALSE	CD7-6B7	Hu	BioLegend	343102
1094	CD85k 165Ho	CD85k, ILT3, LILRB4	165Ho	FALSE	ZM4.1	Hu	BioLegend	333002
1100	HLA-DR 143Nd	HLA-DR	143Nd	FALSE	L243	Hu	DVS-Fluidigm	3143013B

Figure S1

A

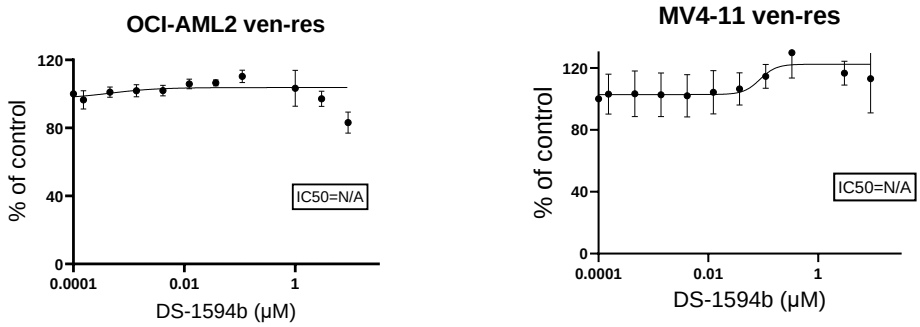

B

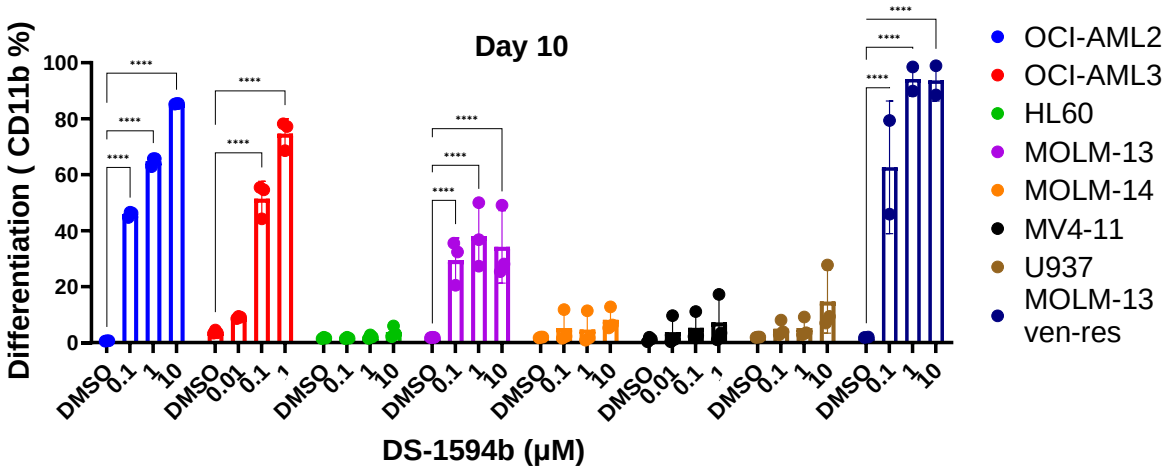

C

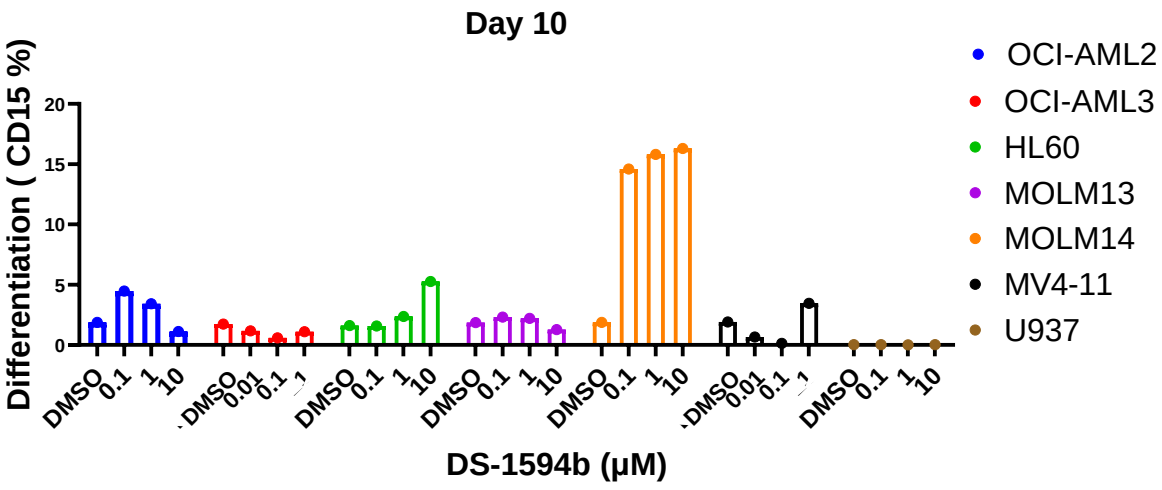

D

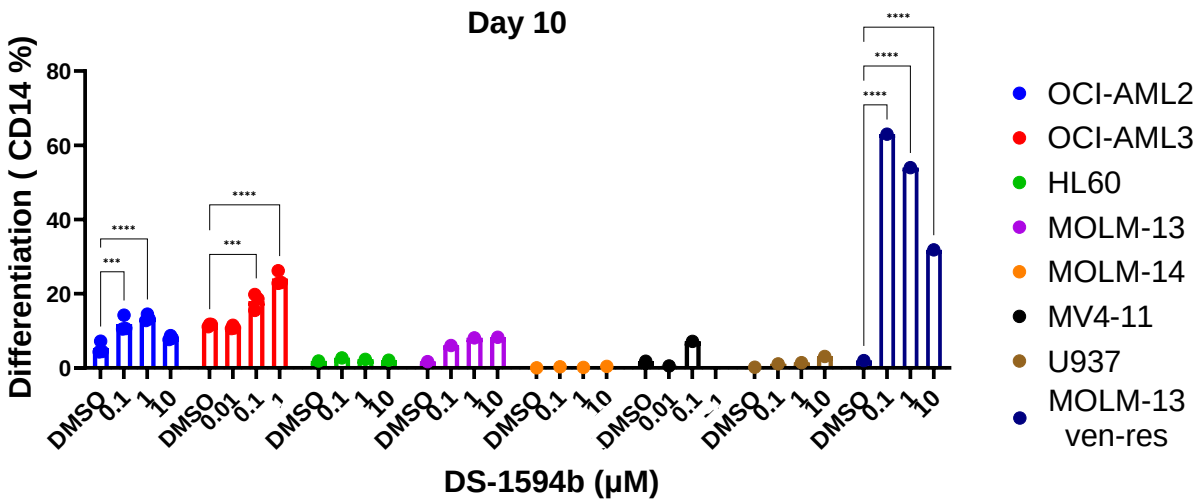

E

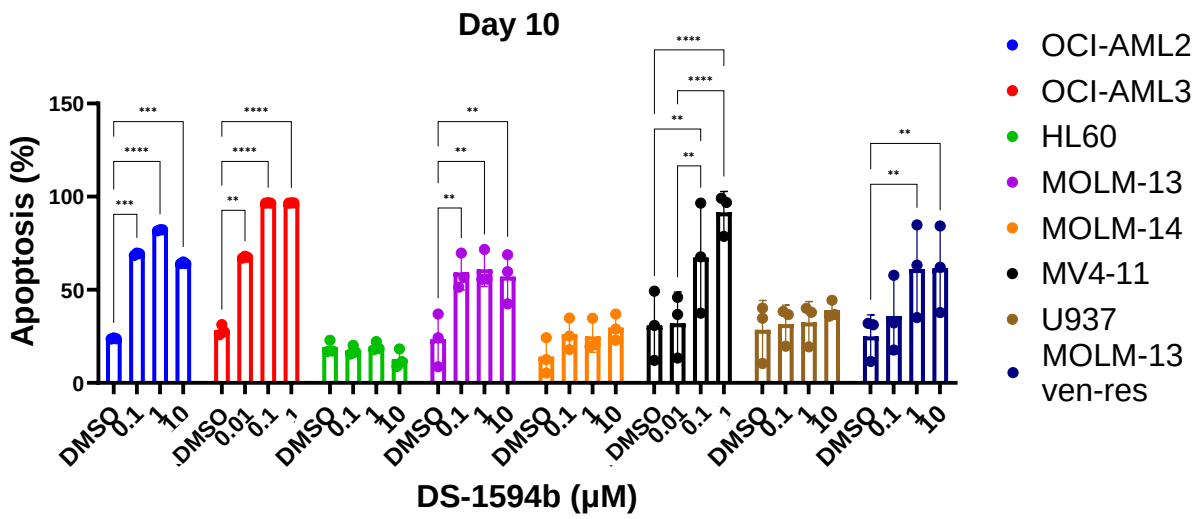

Figure S2

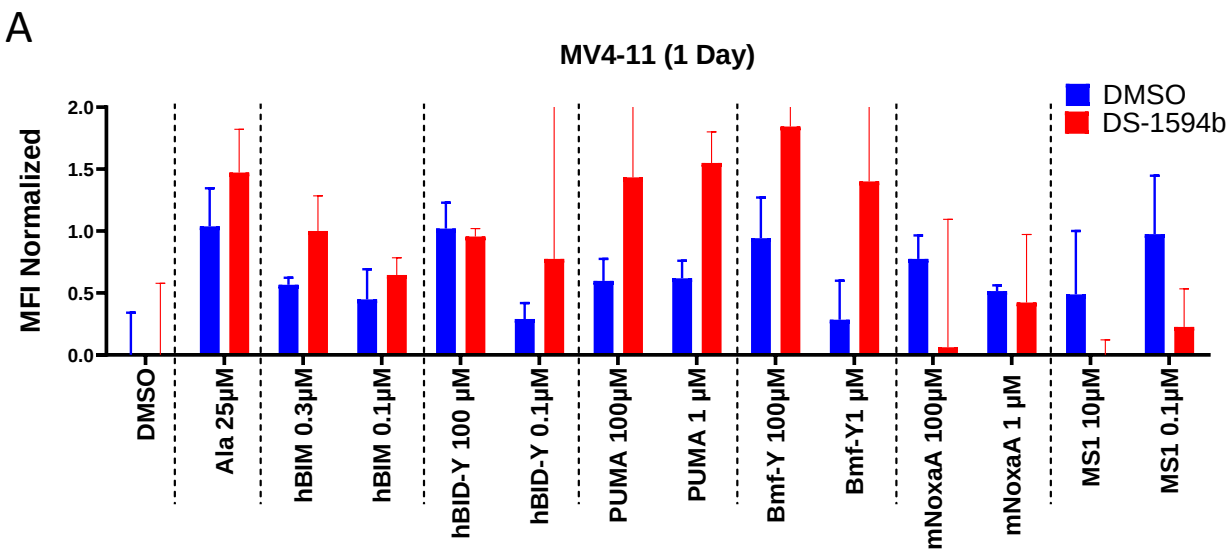
A
MV4-11 (1 Day)
MFI Normalized
DMSO
DS-1594b
DMSO
Ala 25µM
hBIM 0.3µM
hBIM 0.1µM
hBID-Y 100 µM
hBID-Y 0.1µM
PUMA 100µM
PUMA 1 µM
Bmf-Y 100µM
Bmf-Y1 µM
mNoxaA 100µM
mNoxaA 1 µM
MS1 10µM
MS1 0.1µM

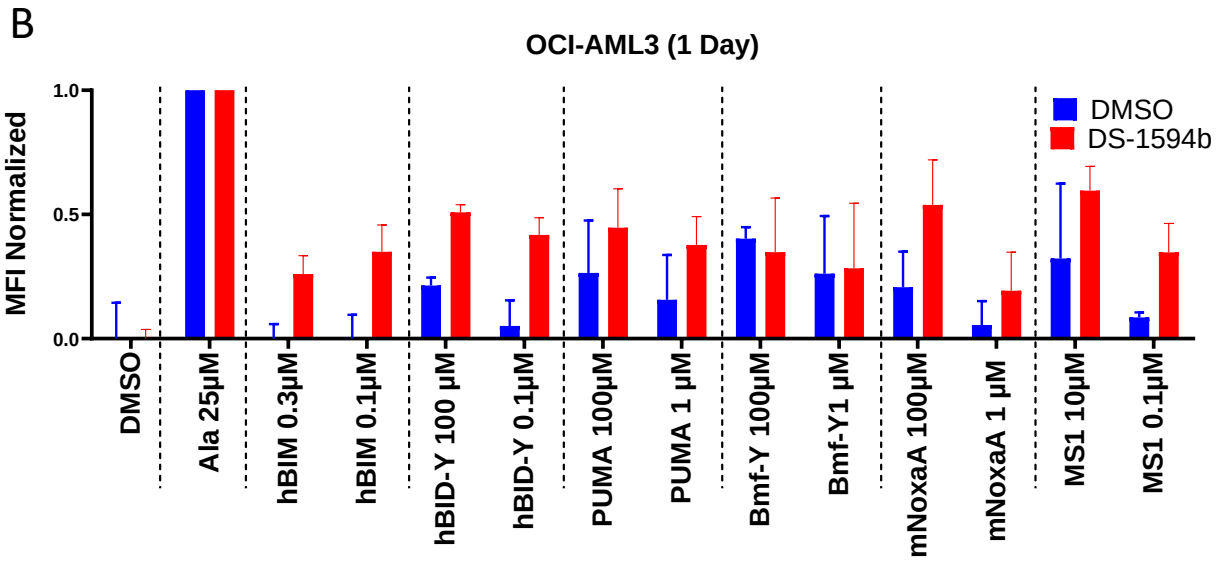
B
OCI-AML3 (1 Day)
MFI Normalized
DMSO
DS-1594b
DMSO
Ala 25µM
hBIM 0.3µM
hBIM 0.1µM
hBID-Y 100 µM
hBID-Y 0.1µM
PUMA 100µM
PUMA 1 µM
Bmf-Y 100µM
Bmf-Y1 µM
mNoxaA 100µM
mNoxaA 1 µM
MS1 10µM
MS1 0.1µM

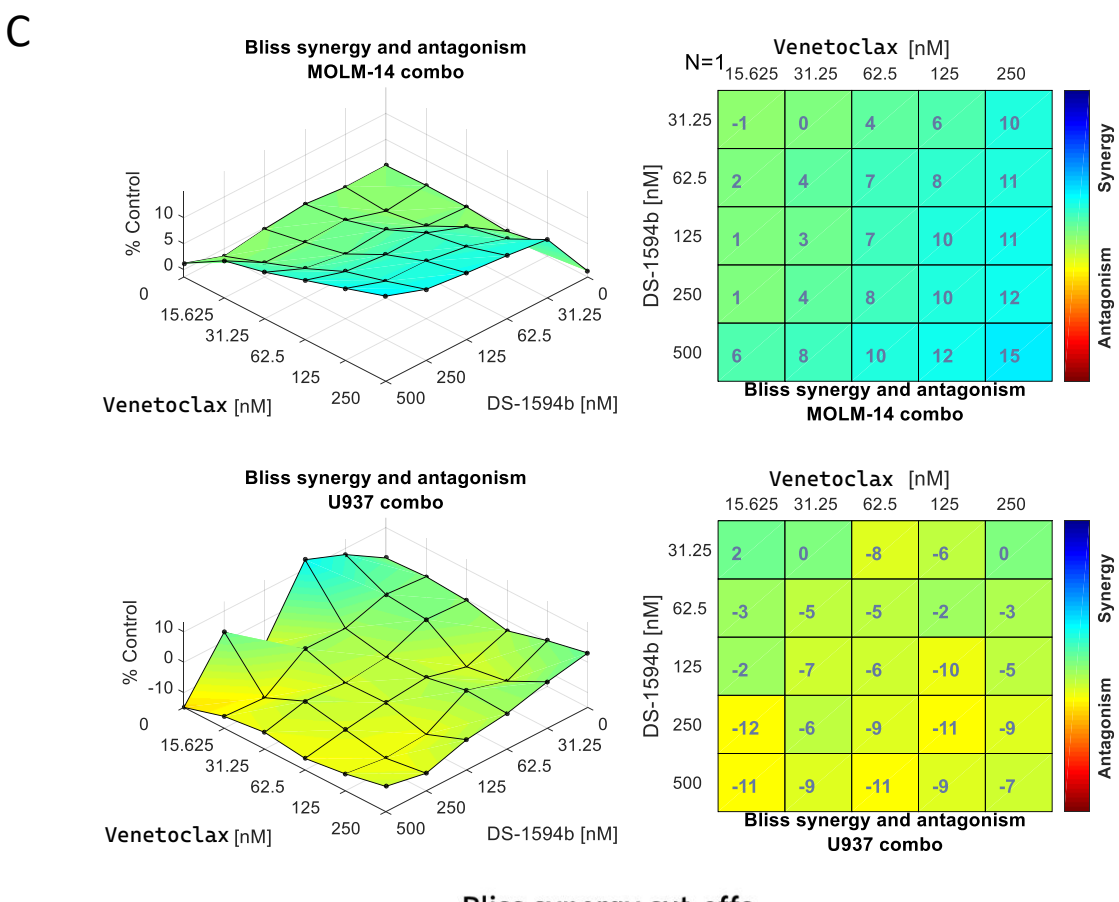
C
Bliss synergy and antagonism
MOLM-14 combo
% Control
Venetoclax [nM]
DS-1594b [nM]
N=1
Venetoclax [nM]
DS-1594b [nM]
Synergy
Antagonism
Bliss synergy and antagonism
MOLM-14 combo
Bliss synergy and antagonism
U937 combo
Bliss synergy and antagonism
U937 combo
Bliss synergy cut-offs
Antagonism
Bliss < −10
Additive
−10 ≤ Bliss ≤ 10
Synergy
Bliss > +10

Figure S3

A

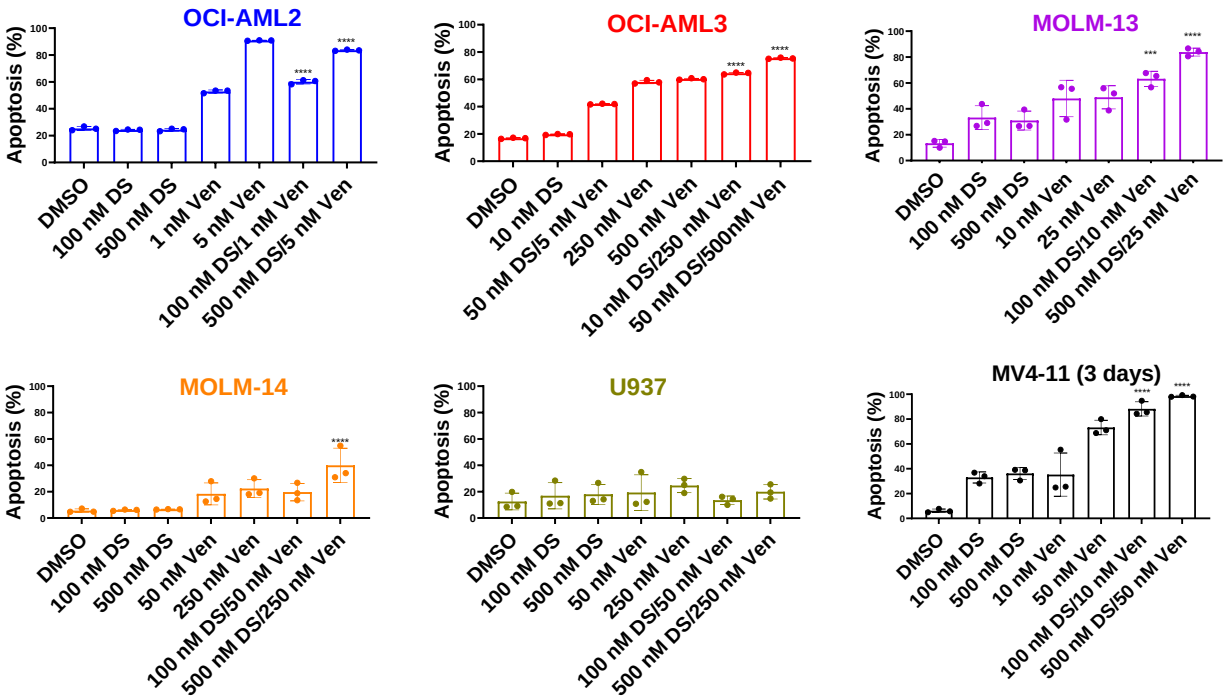
OCI-AML2
Apoptosis (%)
DMSO
100 nM DS
500 nM DS
1 nM Ven
5 nM Ven
100 nM DS/1 nM Ven
500 nM DS/5 nM Ven
OCI-AML3
DMSO
10 nM DS
50 nM DS/5 nM Ven
250 nM Ven
500 nM Ven
10 nM DS/250 nM Ven
50 nM DS/500nM Ven
MOLM-13
DMSO
100 nM DS
500 nM DS
10 nM Ven
25 nM Ven
100 nM DS/10 nM Ven
500 nM DS/25 nM Ven
MOLM-14
DMSO
100 nM DS
500 nM DS
50 nM Ven
250 nM Ven
100 nM DS/50 nM Ven
500 nM DS/250 nM Ven
U937
DMSO
100 nM DS
500 nM DS
50 nM Ven
250 nM Ven
100 nM DS/50 nM Ven
500 nM DS/250 nM Ven
MV4-11 (3 days)
DMSO
100 nM DS
500 nM DS
10 nM Ven
50 nM Ven
100 nM DS/10 nM Ven
500 nM DS/50 nM Ven

Figure S4

A

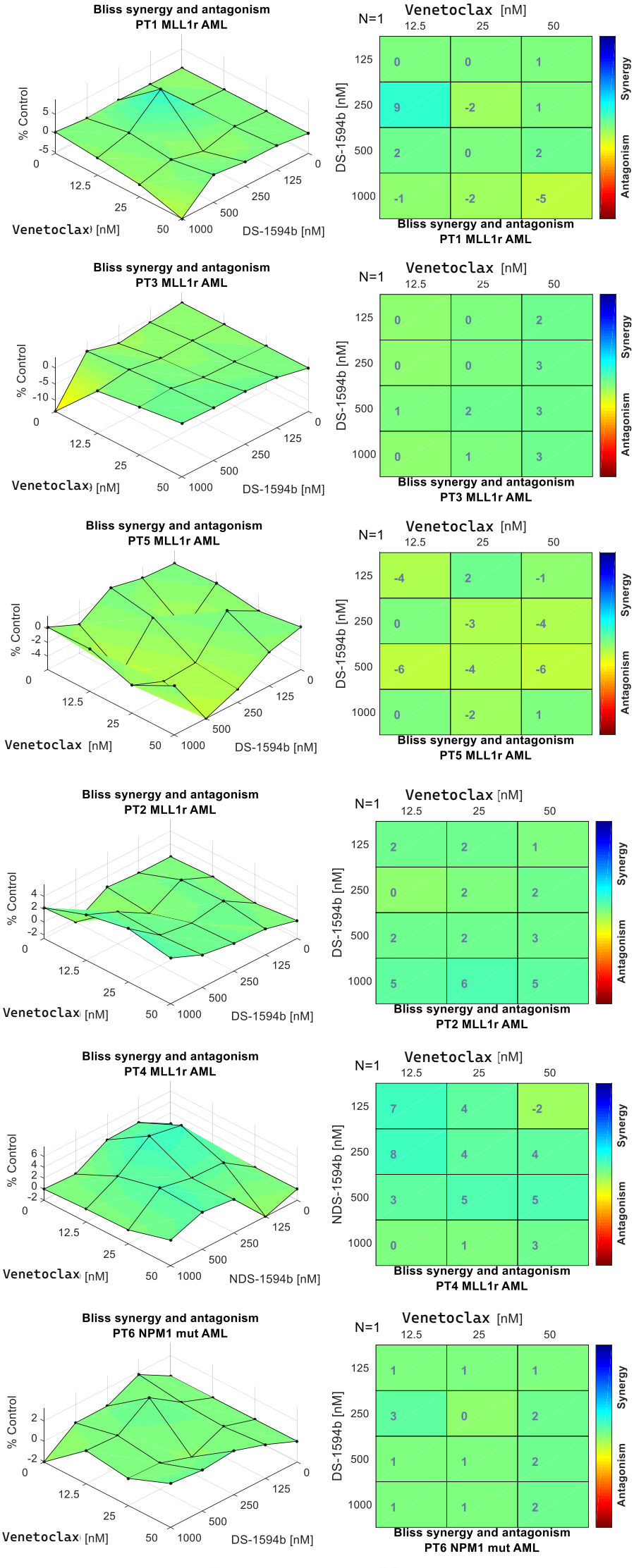
Bliss synergy and antagonism
PT1 MLL1r AML
% Control
Venetoclax [nM]
DS-1594b [nM]
N=1
Venetoclax [nM]
12.5
25
50
125
250
500
1000
DS-1594b [nM]
0 0 1
9 -2 1
2 0 2
-1 -2 -5
Synergy
Antagonism
Bliss synergy and antagonism
PT1 MLL1r AML
Bliss synergy and antagonism
PT3 MLL1r AML
% Control
Venetoclax [nM]
DS-1594b [nM]
N=1
Venetoclax [nM]
0 0 2
0 0 3
1 2 3
0 1 3
Synergy
Antagonism
Bliss synergy and antagonism
PT3 MLL1r AML
Bliss synergy and antagonism
PT5 MLL1r AML
% Control
Venetoclax [nM]
DS-1594b [nM]
N=1
Venetoclax [nM]
-4 2 -1
0 -3 -4
-6 -4 -6
0 -2 1
Synergy
Antagonism
Bliss synergy and antagonism
PT5 MLL1r AML
Bliss synergy and antagonism
PT2 MLL1r AML
% Control
Venetoclax [nM]
DS-1594b [nM]
N=1
Venetoclax [nM]
2 2 1
0 2 2
2 2 3
5 6 5
Synergy
Antagonism
Bliss synergy and antagonism
PT2 MLL1r AML
Bliss synergy and antagonism
PT4 MLL1r AML
% Control
Venetoclax [nM]
NDS-1594b [nM]
N=1
Venetoclax [nM]
7 4 -2
8 4 4
3 5 5
0 1 3
Synergy
Antagonism
Bliss synergy and antagonism
PT4 MLL1r AML
Bliss synergy and antagonism
PT6 NPM1 mut AML
% Control
Venetoclax [nM]
DS-1594b [nM]
N=1
Venetoclax [nM]
1 1 1
3 0 2
1 1 2
1 1 2
Synergy
Antagonism
Bliss synergy and antagonism
PT6 NPM1 mut AML
Bliss synergy cut-offs
Antagonism
Bliss < −10
Additive
−10 ≤ Bliss ≤ 10
Synergy
Bliss > +10

Figure S5

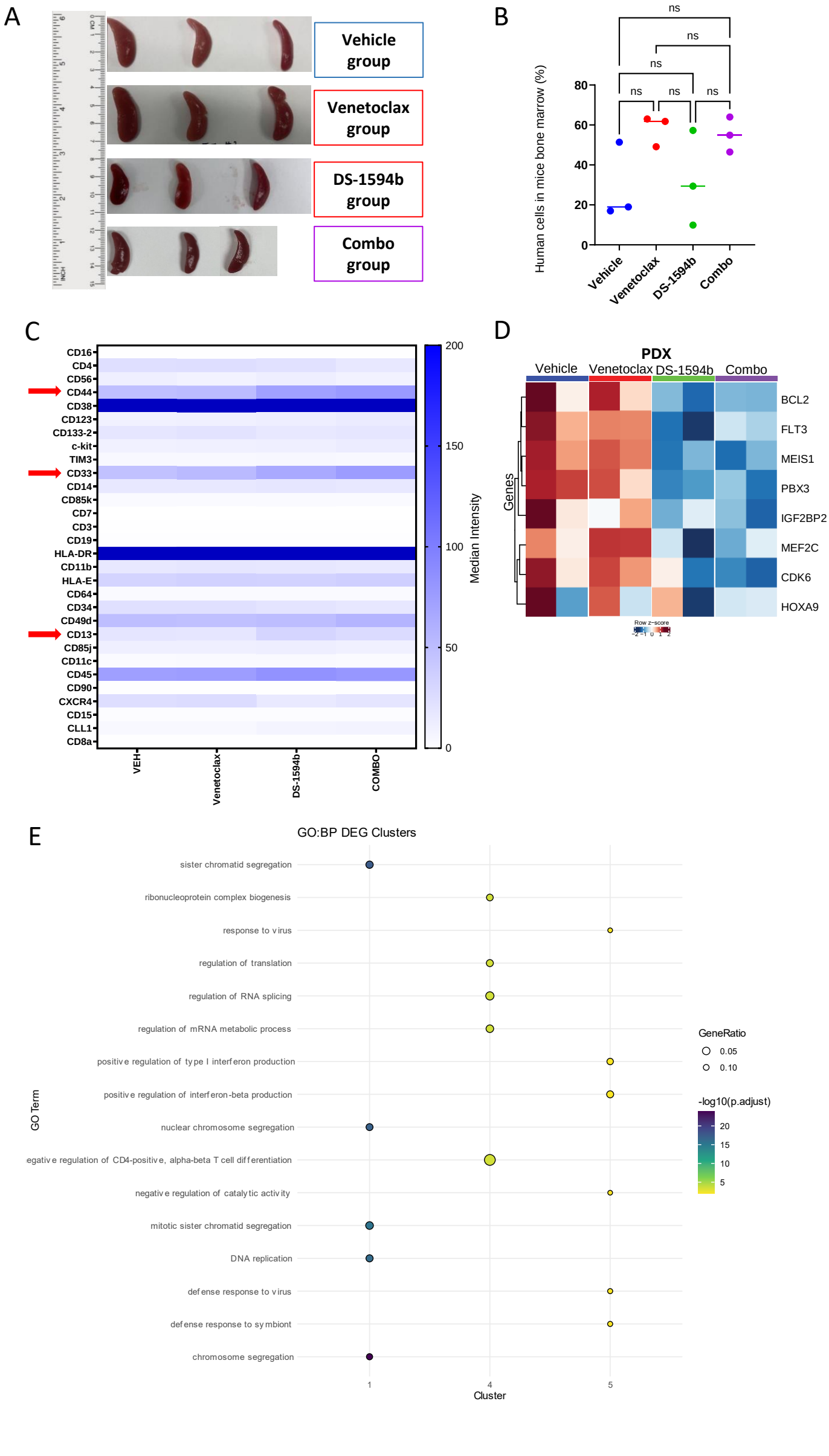
A
Vehicle group
Venetoclax group
DS-1594b group
Combo group
B
Human cells in mice bone marrow (%)
ns
Vehicle
Venetoclax
DS-1594b
Combo
C
CD16
CD4
CD56
CD44
CD38
CD123
CD133-2
c-kit
TIM3
CD33
CD14
CD85k
CD7
CD3
CD19
HLA-DR
CD11b
HLA-E
CD64
CD34
CD49d
CD13
CD85j
CD11c
CD45
CD90
CXCR4
CD15
CLL1
CD8a
VEH
Venetoclax
DS-1594b
COMBO
Median Intensity
200
150
100
50
0
D
PDX
Vehicle
Venetoclax
DS-1594b
Combo
Genes
BCL2
FLT3
MEIS1
PBX3
IGF2BP2
MEF2C
CDK6
HOXA9
Row z-score
E
GO:BP DEG Clusters
sister chromatid segregation
ribonucleoprotein complex biogenesis
response to virus
regulation of translation
regulation of RNA splicing
regulation of mRNA metabolic process
positive regulation of type I interferon production
positive regulation of interferon-beta production
nuclear chromosome segregation
negative regulation of CD4-positive, alpha-beta T cell differentiation
negative regulation of catalytic activity
mitotic sister chromatid segregation
DNA replication
defense response to virus
defense response to symbiont
chromosome segregation
GO Term
1
4
5
Cluster
GeneRatio
0.05
0.10
-log10(p.adjust)
20
15
10
5

Figure S6

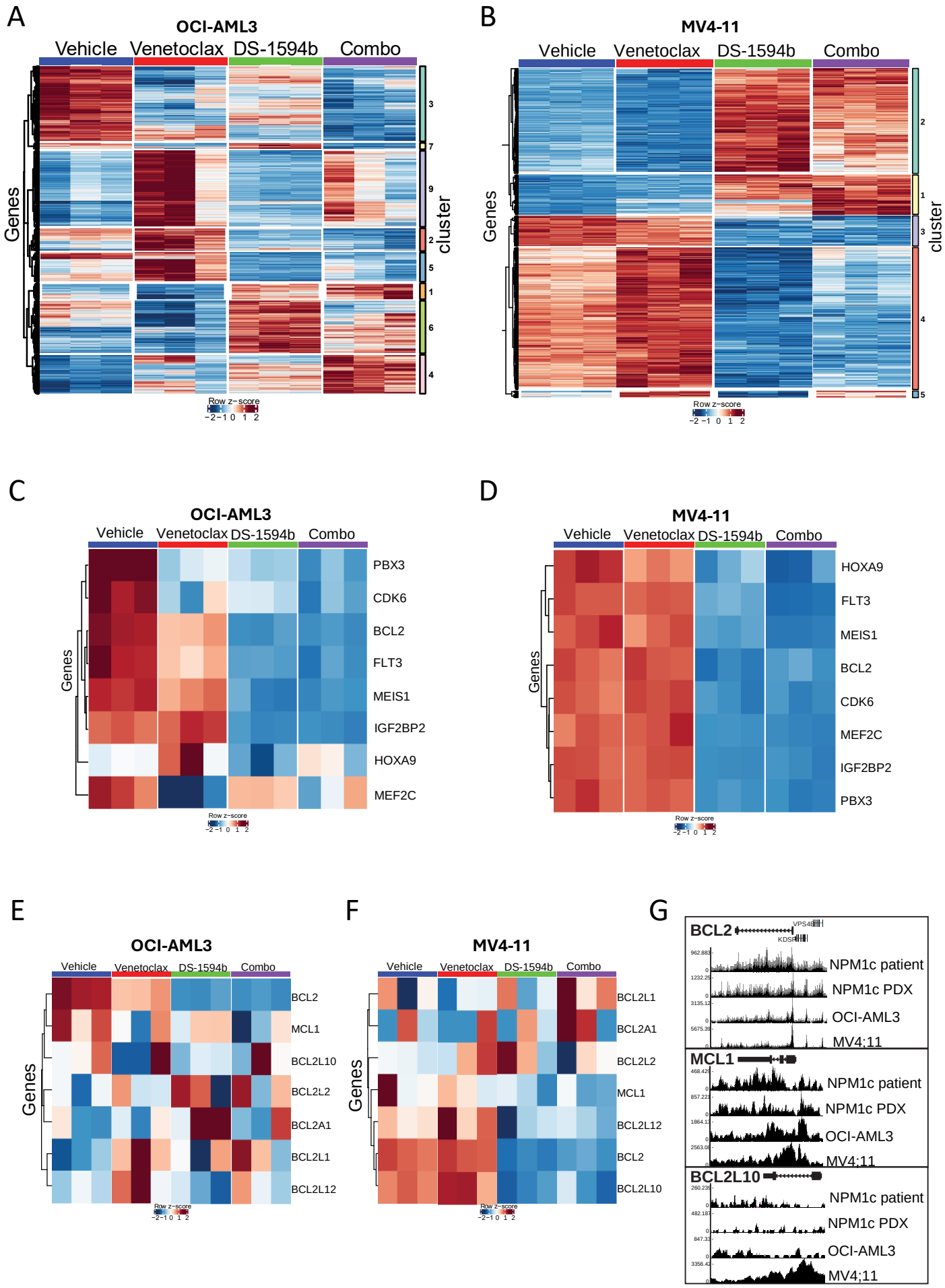
A
OCI-AML3
Vehicle
Venetoclax
DS-1594b
Combo
Genes
cluster
Row z-score
B
MV4-11
C
OCI-AML3
PBX3
CDK6
BCL2
FLT3
MEIS1
IGF2BP2
HOXA9
MEF2C
D
MV4-11
E
OCI-AML3
BCL2
MCL1
BCL2L10
BCL2L2
BCL2A1
BCL2L1
BCL2L12
F
MV4-11
G
BCL2
MCL1
BCL2L10
NPM1c patient
NPM1c PDX
OCI-AML3
MV4;11

Figure S7

A

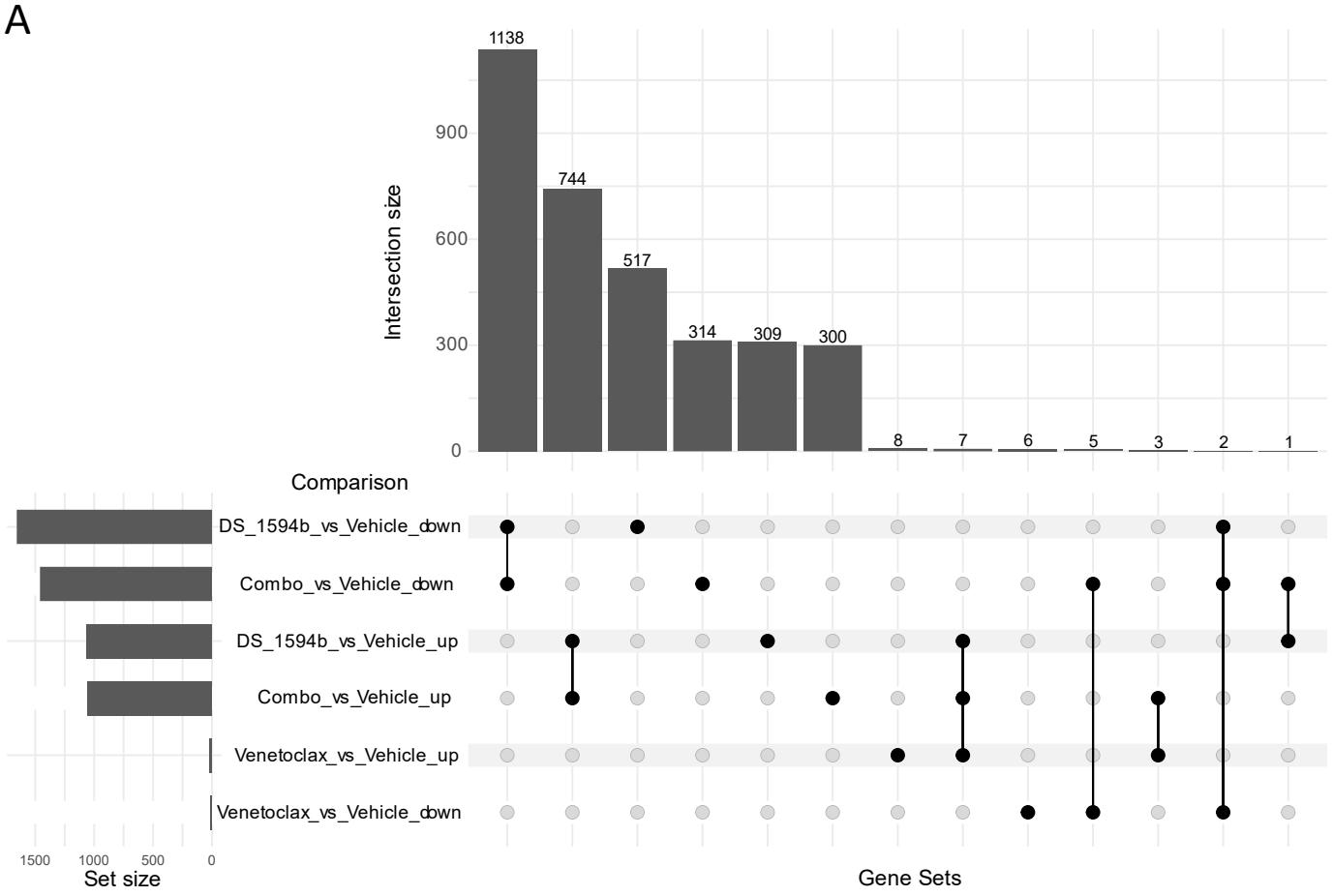
1138
744
517
314
309
300
8
7
6
5
3
2
1
Intersection size
900
600
300
0
Comparison
DS_1594b_vs_Vehicle_down
Combo_vs_Vehicle_down
DS_1594b_vs_Vehicle_up
Combo_vs_Vehicle_up
Venetoclax_vs_Vehicle_up
Venetoclax_vs_Vehicle_down
1500
1000
500
0
Set size
Gene Sets

Supplementary Table 1. Antibodies used for Western blot analysis.

Supplementary Table 2. Antibodies used for CyTOF analysis.

Supplementary Figure 1. Effects of treatment with DS-1594b alone and in combination with venetoclax on various cell lines.

A. Proliferation assays were conducted by treating OCI-AML2 ven-res and MV4-11 ven-res cell lines for 7 days with DS-1594b alone at the indicated concentrations. Dose-response curves were analyzed using a curve-fitting routine based on nonlinear regression to compute the IC_{50} value. **B.** Cell lines were treated with vehicle (0.2% DMSO) or 0.1, 1, or 10 μM (or 0.01, 0.1, and 1 μM) DS-1594b for 10 days. Differentiation effects were determined by flow cytometry using the CD11b marker. Two-way ANOVA was performed to determine statistical significance (* $P < 0.05$; ** $P < 0.01$; *** $P < 0.001$; ****$P < 0.0001$). **C.** Differentiation effects in all cell lines was determined by flow cytometry using the CD15 marker. Two-way ANOVA was performed to determine statistical significance (* $P < 0.05$; ** $P < 0.01$; *** $P < 0.001$; ****$P < 0.0001$). **D.** Differentiation effects in all cell lines were determined by flow cytometry using the CD14 marker on all cell lines. Two-way ANOVA was performed to determine statistical significance (* $P < 0.05$; ** $P < 0.01$; *** $P < 0.001$; ****$P < 0.0001$). **E.** Apoptosis assay was conducted by treating cell lines for 10 days with the indicated concentrations. Apoptotic cells were determined by flow cytometry using counting beads, Annexin V, and DAPI. Two-way ANOVA was performed to determine statistical significance (*, $P < 0.05$; **, $P < 0.01$; ***, $P < 0.001$; ****, $P < 0.0001$).

Supplementary Figure 2. BH3 profiling and bliss synergy scores in cell lines treated with Venetoclax and/or DS-1594b.

A. MV4-11 and **B.** OCI-AML3 cell lines were treated for 24 hours and analyzed for BH3 profiling. Cells were then permeabilized with digitonin and exposed to BH3 peptides (hBIM, hBID-Y, PUMA,

Bmf-Y, mNoxaA, MS1; synthesized by New England Peptide). The mitochondrial transmembrane potential loss was monitored by cytochrome C release. DMSO and Ala were used as the negative and positive controls, respectively, for cytochrome C release. MFI Normalization was calculated following this equation: 1-(MFI(log)-(DMSO-Ala)/(DMSO-Ala). **C.** U937 and MOLM-14 were treated with the indicated concentrations of DS-1594b and venetoclax for 5 days. Bliss synergy scores of the combination treatment on cell lines were determined using Combenefit software 2.0. Values > +10 indicate synergy, between -10 and +10 indicate additive effects, and < -10 indicate antagonism.

Supplementary Figure 3. Apoptosis assay on AML cell lines after treatment with DS-1594b in combination with venetoclax

A. Cell lines listed above were treated with vehicle (0.2% DMSO) or 0.1, 1, or 10 μM (or 0.01, 0.1 and 1 μM) DS-1594b for 5 days. Differentiation effects were determined by flow cytometry using the CD11b marker. Two-way ANOVA was performed to determine statistical significance (* $P < 0.05$; ** $P < 0.01$; *** $P < 0.001$; ****$P < 0.0001$).

Supplementary Figure 4. Bliss synergy scores of AML patient samples treated with DS-1594b and Venetoclax.

A. Patient samples were treated with the indicated concentrations of DS-1594b and venetoclax for 3 days. Bliss synergy scores of the combination treatment on cell lines were determined using Combenefit software 2.0. Values > +10 indicate synergy, between -10 and +10 indicate additive effects, and < -10 indicate antagonism.

Supplementary Figure 5. Effects of treatment with DS-1594b and Venetoclax on PDX mouse model.

A. Photographs of the spleens from three mice within each treatment group. **B.** Percentage of human cells in the bone marrow of three mice from each treatment group. **C.** The expression

levels of each protein within every treatment group. **D.** Heatmaps showing z-scored expression of canonical Menin-MLL transcriptional target genes following treatment with Venetoclax, DS-1594b, or a combination, in PDX cells. **E.** GO:BP analysis, filtered to the top 5 significantly enriched terms, in the clusters of differentially expressed genes in the PDX model. Cluster numbers refer to the clusters in Fig. 5A.

Supplementary Figure 6. Effects of treatment with DS-1594b and Venetoclax on AML cell lines.

A. Clustered heatmaps of differentially expressed genes following treatment with Venetoclax, DS-1594b, or a combination, in OCI-AML3 cells. **B.** Clustered heatmaps of differentially expressed genes following treatment with Venetoclax, DS-1594b, or a combination, in MV4-11 cells. **C.** Heatmaps showing z-scored expression of canonical Menin-MLL transcriptional target genes following treatment with Venetoclax, DS-1594b, or a combination, in OCI-AML3. **D.** Heatmaps showing z-scored expression of canonical Menin-MLL transcriptional target genes following treatment with Venetoclax, DS-1594b, or a combination, in MV4-11. **E.** Clustered heatmaps showing z-scored expression of anti-apoptosis genes following treatment with Venetoclax, DS1594b, or a combination, in OCI-AML3. **F.** Clustered heatmaps showing z-scored expression of anti-apoptosis genes following treatment with Venetoclax, DS-1594b, or a combination, in MV4-11 cells. **G.** Menin ChIP-seq and ChIpmentation in OCI-AML3 and MV4-11 cells and small cell number ChIPmentation for Menin in an NPM1-mutant primary AML patient sample and an NPM1-mutant PDX sample at the promoters of key anti-apoptotic genes. MV4-11 data were obtained from publicly available GEO dataset GSE196036.

Supplementary Figure 7. Upset plot in PDX model.

A. Upset plot comparing significant (p.adj <0.05) up-regulated and down-regulated genes across treatment conditions in PDX model.